UNDERSTANDING THE RELATIONSHIP BETWEEN AGRICULTURAL NUTRIENTS NPS, LAND MANAGEMENT, AND CLIMATE USING DISTRIBUTED HYDROLOGIC MODELS

BY

CONGYU HOU

DISSERTATION

Submitted in partial fulfillment of the requirements
for the degree of Doctor of Philosophy in Agricultural and Biological Engineering
in the Graduate College of the
University of Illinois Urbana-Champaign, 2021

Urbana, Illinois

Doctoral Committee:

Associate Professor Maria Librada Chu, Chair
Professor Yuanhui Zhang
Professor Praveen Kumar
Dr. Kevin Armstrong, John Deere Technology and Innovation Center

Abstract

The use of chemical fertilizer has enhanced agricultural production that helped provide food to seven billion people worldwide. Particularly, the use of nitrogen (N) and phosphorus (P) fertilizers, which increased more than nine and four times, respectively, during the last five decades, played significant roles in improving soil fertility, crop health, and yield performance. However, the massive use of N and P fertilizer has led to severe environmental issues such as harmful algal bloom (HAB), decline in biodiversity, and contaminated drinking water which can lead to serious threats to public health and critical stress to the agroecosystem because of the high fertilizer loss. To mitigate the excessive nutrient loading in our water bodies, different land management schemes have been developed and implemented to reduce N and P NPS in the agroecosystem, but the effectiveness of these land management practices needs evaluation. Due to the complexity of the watershed response to natural and anthropogenic stressors like changing climate and changes in land management scenarios, a modeling framework that allows the conceptualization of physically based hydrologic and transport processes should be adopted to provide reliable predictions and better understanding of the systemic responses. This study was geared at understanding how agricultural nutrients NPS were impacted by natural and anthropogenic changes such as climate and land management practices, respectively. Modeling frameworks with field-level spatial resolution were developed to evaluate the effectiveness of NPS reduction practices when detailed and field-level specific land management practices were implemented under extreme climate projections. First, the impacts of different land management practices and climate on surface runoff linked N load at the field-level scale were evaluated. Second, different types of N NPS patterns in the Upper Sangamon River Basin (USRB), a highly cultivated watershed, under wet and dry future climate projections were compared when

implementing different land management practices at the field-level scale. Finally, the risks of HAB occurrence and the effectiveness of different land management practices in mitigating this risk under extreme climate projections were assessed. Our results showed that fertilizer application rate was the most critical factor in determining both the amount and the probability of high *N* load. If 50% less fertilizer was applied in a highly cultivated watershed focusing on growing corn and soybean, the nitrate concentrations were expected to remain lower than the United States Environmental Protection Agency (EPA) and World Health Organization (WHO) limit even under extreme climate projections. Other possible land management practices that could also reduce N concentration and load included the target application management approach, crop rotation using alfalfa, and cover cropping with winter wheat. Ammonia and nitrite transformed from nitrate fertilizer, however, were not expected to become an environmental concern in the USRB under climate projections. Furthermore, P was found to be the limiting nutrient despite an important P point-source in the USRB. In cases like this, land management practices focusing on P reduction should be adopted when HAB or GAB occurrences are a concern and N reduction practices should be applied to the USRB if downstream HAB or GAB occurrence risks were high.

With the improved understanding of the relation between agricultural nutrients NPS and natural and anthropogenic stressors, more specific and effective land management practices targeting the reduction of agricultural nutrients NPS could be applied based on different climate and natural environment characteristics. Additionally, our projects also provided two modeling frameworks focusing on simulating the different agricultural nutrients NPS considering the field level processes. These frameworks can provide a better platform in evaluating the effectiveness of different land management practices in reducing agricultural nutrients NPS. Overall, my research

enabled other researchers and decision makers to assess environmental issues risks and compare the tradeoffs between the welfare of agro-ecosystems and economic benefits using models that are closer to reality than empirical models that have been widely used currently.

Acknowledgements

I would like to use this opportunity to express my sincere thanks to my advisor, Dr. Maria L. Chu and her husband, Dr. Jorge Alberto Guzman Jaimes, for all the support provided during the last seven years. Your parents-like support not only guided me through my master and PhD degree, but also taught me how to live a life in the U.S. I could not imagine the difficulties that I might encounter during my stay in the U.S. without your support and help.

I would also like to thank my doctoral committee members: Professor Yuanhui Zhang, Professor Praveen Kumar, and Dr. Kevin Armstrong. Your expertise in different areas and kind suggestions and helps contributed significantly to this project. Your valuable feedbacks polished my projects and your comments encouraged me to become a better me in research.

Trees can only survive with their soil and my soil is the love of my families and friends. Your love and care have been helping and will still be helping me through all the difficulties in my life. All words are powerless when compared to the love I have been given. Here at the moment, I hope all my beloved are happy and healthy.

TABLE OF CONTENTS

INTRODUCTION

The use of chemical fertilizer has enhanced agricultural production that helped provide food to seven billion people worldwide. Particularly, the use of nitrogen (N) and phosphorus (P) fertilizers, which increased more than nine and four times, respectively, during the last five decades, played significant roles in improving soil fertility, crop health, and yield performance (Lu and Tian, 2017). However, the massive use of N fertilizer has led to severe environmental issues and critical stress to the agroecosystem due to the fact that over 25% of the total N applied is lost via leaching and surface runoff (Smil, 1999). Approximately $4\ x\ 10^{13}$ grams of N are being transported annually from farmlands to river bodies mainly through leaching and surface runoff. The high amount of N loss led to environmental issues including harmful algal bloom (HAB), decline in biodiversity, and contaminated drinking water which can lead to serious threats to public health (Nakaji et al., 2001; Oenema and Roest, 1998; Timmons et al., 1973). On the other hand, excessive P load in our water bodies can trigger the occurrence of HAB more likely than any other types of agricultural nutrients in fresh water systems (Carvalho et al., 2013) since P is generally the limiting factor for HAB. To control and reduce the negative effects from N and P loads in our water bodies, different environmental projects have been carried out globally. For example, both N and P nonpoint source (NPS) pollution were critical part of the ongoing national environmental project, "The Gulf Hypoxia Action Plan" (Mississippi River/Gulf of Mexico Watershed Nutrient Task Force, 2008). In this project, the U.S. Environmental Protection Agency (U.S. EPA) has targeted a 15% decrease in nitrate N load and 25% in total phosphorus by 2025 as phase one milestones and a 45% decrease in both nitrate N and total phosphorus load in the Mississippi River basin as ultimate goal, which were also the

long-term reduction goal of upstream states contributing to the basin (e.g. Illinois Nutrient Loss Reduction Strategy) (Wilhite et al., 2015).

To mitigate the excessive nutrient loading in our water bodies, different land management schemes have been developed and implemented to reduce N and P NPS in the agroecosystem. For example, the use of cover crops was reported to reduce leaching and surface runoff and consequently N and P NPS from agricultural field (Dinnes et al., 2002; Unger and Vigil, 1998). Crop rotation, which usually referred to corn-soybean two-year crop rotation practice in the North America Corn Belt, has a significantly positive effect on soil quality indicators including total organic carbon, bulk density, soil pH, total N, and extractable P and K (Dinnes et al., 2002). In addition, changing application timing from fall to spring and separating annual application into halves were proven to be potential positive land management practice to reduce N and P NPS (Dinnes et al., 2002).

To evaluate the effectiveness of the land management practices, numerical models are being used to determine the expected spatial and temporal changes in N and P loads resulting from these practices. However, since most of the numerical environmental models currently available to simulate the fate and transport of N and P are lumped at the sub-basin level, they cannot provide information for field-level analysis where these practices are being implemented. The failure to consider these factors can lead to inappropriate agricultural nutrients NPS reduction practices to be implemented causing potential risk including decrease in yield, more NPS losses, or even decline in biodiversity of the agroecosystem. Furthermore, most of the conceptual models widely used in environmental simulations used parameters that do not have any physical meaning and can only be obtained through calibration. Using parameters that do not represent physical

properties or processes can lead to unrealistic representation of the system resulting in high levels of uncertainty.

To address these gaps, a modeling framework with field-level spatial resolution was necessary to evaluate the effectiveness of NPS reduction practices if detailed and field-level specific land management practices were implemented. Furthermore, the numerical models should include a comprehensive simulation of water and nutrient movements to better understand the relationship between agricultural nutrients NPS and different land management practices under different climate projections. The overall goal of this research was to improve our understanding of how agricultural nutrients NPS were impacted by natural and anthropogenic changes such as climate and land management practices, respectively. To accomplish this goal, three specific objectives were developed into independent chapters as follows:

Objective 1:

Evaluate the impacts of the different land management practices and climate on surface runoff linked N load at the field-level scale.

(a) Develop a framework using the integrated Pesticide Root Zone Model version 3 (PRZM) for the Willow Creek Watershed in central western Oklahoma to analyze changes in N load in surface runoff at a high spatial-temporal resolution under high greenhouse emission climate projections;

(b) Determine the effects from the combination of factors that can lead to a long-term high N load including different crop rotation schemes, different fertilizer application schemes, and projected climate scenarios using the model framework developed in section (a);

Objective 2:

Compare the different types of N NPS patterns in a highly cultivated watershed under wet and dry future climate projections when implementing different land management practices at the field-level scale.

(a) Develop a fully distributed physical-based hydrologic model, MIKE SHE, and a hydrodynamic river model, MIKE 11, coupled with ECO-Lab to simulate the fate and transport of different forms of N in the agro-ecosystem of the Upper Sangamon River Basin (USRB), a highly cultivated watershed in central Illinois;

(b) Determine the nitrate, nitrite, and ammonia NPS temporal and spatial patterns under different climate projections and land management practices scenarios;

(c) Assess the risks of exceeding the safe environmental limit for nitrate, nitrite, and ammonia NPS under different management practices and future climate projections.

Objective 3:

Assess the occurrence risk of HAB occurrence in a highly cultivated watershed and evaluate the effectiveness of different land management in mitigating this risk under future climate projections.

(a) Develop an Eco-Lab model to simulate the fate and transport of phosphorus coupled with MIKE SHE and MIKE 11 models for the USRB;

(b) Establish the HAB occurrence risk range by simulating N and P concentrations time series along the river under extreme climate projections;

(c) Assess the effectiveness of reduced fertilizer application rates in reducing agricultural nutrients NPS related HAB under extreme future climate changes.

CHAPTER 1: FIELD SCALE NITROGEN LOAD IN SURFACE RUNOFF: IMPACTS OF MANAGEMENT PRACTICES AND CHANGING CLIMATE.[1]

Introduction

The Haber-Bosch process developed in the 20th century brought production of Nitrogen (*N*) fertilizer to industrial scales, boosting crop production but with the consequence of exacerbating *N* losses from agricultural landscapes. In fact, studies reported that the *N* fertilizer loss via surface runoff and leaching processes can account for up to 1/3 and 3/4 of the total *N* applied (Douglas Jr. et al., 1998) and can further increase during unusual rainfall events following fertilizer application. *N* losses decrease *N* fertilizer application efficiency (Turner, 2004) prompting increase in application rates to maintain crop productivity, which will consequently, increase the *N* load in our water bodies. High *N* load can also stem from a combination of numerous causes. Researchers found that higher fertilizer application amount, shallow application depth, and fewer application times would largely increase *N* load from cultivated landscapes (Douglas Jr. et al., 1998; Timmons et al., 1973). Topography is a significant factor that can lead to serious *N* load. Farmlands with slopes greater than 15 degrees are not suitable for agricultural activities due to high erosion rate and *N* load during rainfall events (Chen et al., 2003). Land management practices that can prevent high *N* load are constantly being sought for mitigation and conservation purposes. For instance, researchers found that the total *N* load in rivers could be reduced by decreasing the *N* application in the area near watershed outlets (Schilling and Wolter, 2009).

[1]Hou, C., Chu, M. L., Guzman, J. A., Triana, J. S. A., Moriasi, D. N., & Steiner, J. L. (2019). Field scale nitrogen load in surface runoff: Impacts of management practices and changing climate. Journal of environmental management, 249, 109327.

Quantifying the impacts of different agricultural activities on *N* load requires continuous monitoring of surface runoff and *N* concentration over a long period to determine the spatio-temporal responses of the system to these activities. In addition, to acquire a high spatial resolution dataset, numerous monitoring stations are needed to capture the variability of the different physio-chemical processes in the system. Nonetheless, assessing the impacts of these activities is challenging due to the difficulty of identifying the factors or combination of factors that result in high *N* load. The *N* that ends up in our water bodies is driven by a combination of different agricultural activities and soil properties under the influence of the prevailing weather. Due to the challenges in carrying out long-term field experiments to predict the impacts of prevalent agricultural activities and the variability of weather systems on *N* load, numerical models have been widely implemented. In particular, models quantifying the impacts of different land management practices on *N* load have been numerous in the last decades (Y. Wang et al., 2018). For instance, the Soil Water Assessment Tool (SWAT) is a widely used model in evaluating the impacts of different land management practices on nutrients and sediments (Y. Wang et al., 2018). Like SWAT, the Agricultural Policy Environmental Extender (APEX) model also determines changes in water quality and quantity due to different agricultural activities that span from cropping to animal grazing (Tuppad et al., 2010; Williams et al., 2015). Similarly, the Model for *N* and Carbon (MONICA) predicts changes in *N* load from different land management practice and climate variations (Nendel et al., 2011).

Although these models are able to generally predict the impacts of agricultural activities on *N*, some limitations hinder their effectiveness in assessing field scale spatio-temporal variation in *N*. SWAT and APEX, for example, both perform simulations on sub-basin or watershed levels (Schilling and Wolter, 2009; Tuppad et al., 2010). Since land management practices are typically

implemented at the local scale, the ability of these numerical models to assess changes in *N* at this scale is crucial. Furthermore, most model applications mainly focus on the growing seasons under average rainfall events without considering the uncertainties brought about by future climate (Schilling and Wolter, 2009). Since rainfall is the main driver of surface runoff that facilitates *N* losses to water bodies, assessing *N* load during rainfall events in a probabilistic manner is necessary.

The main objective of this study was to evaluate the impacts of the different land management practices and climate on surface runoff linked *N* load at the field scale level. We developed a framework to analyze changes in *N* load in surface runoff at a high spatio-temporal resolution under high greenhouse emission climate projections.

Specifically, we determined the combination of factors that can lead to a long-term high *N* load under different crop rotation schemes, different fertilizer application schemes, and projected climate scenarios. To accomplish these objectives, a high spatio-temporal modeling framework using the integrated Pesticide Root Zone Model version 3 (PRZM) (Suárez, 2005) was developed for the Willow Creek Watershed in central western Oklahoma to simulate changes in *N* load in surface runoff. By being able to identify the factors that lead to high *N* load losses at a field scale level under different climate projections, focused conservation and mitigation practices can be implemented to minimize the environmental impacts of agricultural activities.

Materials and Methods

Study Area

The Willow Creek Watershed (WCW), with an area of 85.2 km^2, is one of the sub-watersheds of the Fort Cobb Experimental Watershed (FCREW) (Figure 1.1b), which is part of the Central Great Plains Ecoregion located in central western Oklahoma (Figure 1.1a). With a yearly average

temperature of 16°C and an annual precipitation of 889 mm, the WCW has a growing season of over 200 days (University of Oklahoma, 2017). The warm and mild climate in WCW allows the growing of a variety of crops as well as pasture. Based on the U.S. Department of Agriculture (USDA) National Agricultural Statistics (NASS) (USDA, 2019) Cropland Data Layer from Natural Resources Conservation Service (NRCS), about 90 percent of the area in the watershed was used for agriculture from 2006 to 2015 (NRCS, 2017). The main agricultural crops in WCW that require fertilizer were Winter Wheat (31%), Cotton (5%) and other crops that include small percentages of Sorghum and Peanuts, while Pasture (38%) is used for animal grazing. As a result, *N* load from agricultural lands has become the main source of nonpoint source pollution in WCW. In addition, large amounts of cultivated land in this watershed has introduced other environmental problems including impaired water by fecal bacteria from animal grazing and excessive sediment load (Jamieson et al., 2003; Williams, 1975).

The Pesticide Root Zone Model

The PRZM was used to simulate the fate and transport of *N* in the WCW. PRZM is a one-dimensional, dynamic, compartmental model for use in simulating chemical movement, transformation, and fate in the unsaturated soil systems within and immediately below the plant root zone (Suárez, 2005). The inputs of the PRZM included soil properties, land use, land management practices, and climate data while streamflow and *N* load were used to verify the performance of the model in simulating *N* fate and transport (Figure 1.1c). The outputs of the PRZM that were of interest in this study included surface runoff (cm day^{-1}) and *N* load in surface runoff (g day^{-1} m^{-2}).

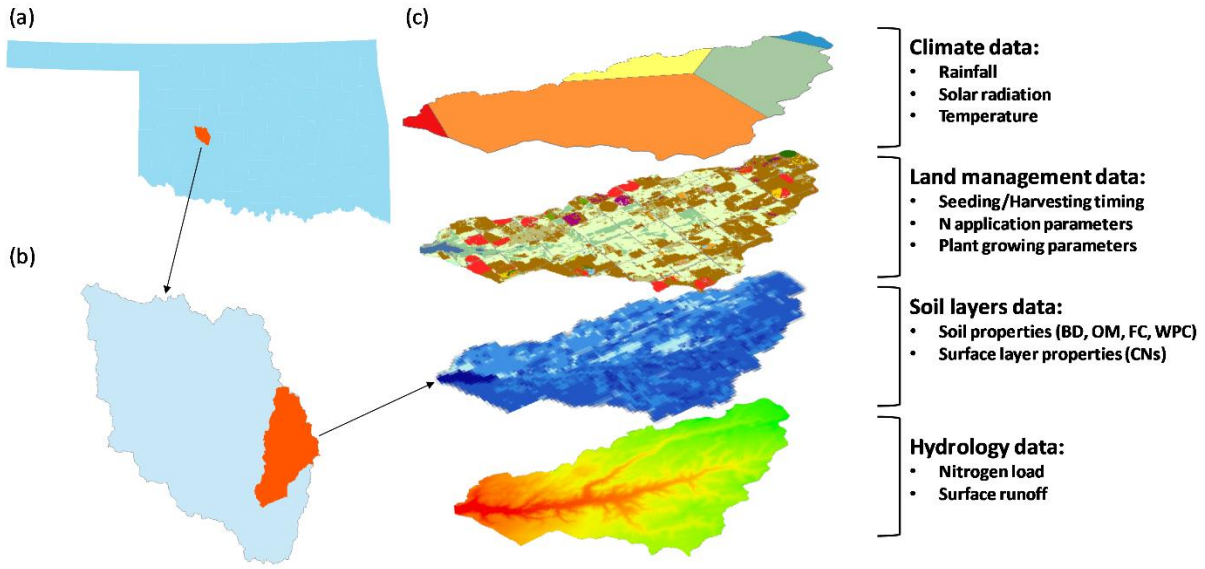

Figure 1.1. (a) The FCREW in Oklahoma; (b) The WCW in FCREW; (c) Data layers used in PRZM, including climate data from five stations, land management data, soil layers data, and hydrology data.

Spatial discretization and model parameterization

Spatial discretization. The baseline model for the WCW was constructed from a structured grid with a 120 x 120 m cell size which lumped responses at each cell was estimated by a PRZM model for a total of 5,911 PRZM models. The time of concentration in WCW was estimated using the Soil Conservation Service (SCS) method to be 12.5 hours (USDA, 2010) . Since the time of concentration was less than one day, it was assumed that the flow and nutrient in all the cells will reach the outlet of the watershed at the end of each time step. Thus, the model outputs at the WCW outlet (i.e., streamflow and *N* load) were computed as the summation of the 5,911 PRZM outputs. To represent the spatial variability of the climate, soil, and crop management, each PRZM model was individually parameterized with soil properties, land use, and management operations derived from soil databases (e.g. SSURGO), and climate and crop management scenarios. The baseline model was then set-up using the historic climate, land use,

and management data to simulate the daily streamflow and *N* load from 2006 to 2015. Projected models were simulated for the period 2020 to 2070, and simulations were performed considering a 100-cm soil profile divided into 6 layers of 5-, 15-, and four 20-cm thickness from top to bottom.

Soil Data and land use. The soil data used in this study was collected and processed from the Soil Survey Geographic Database (USDA, 2017). A variety of soil data used in the model included bulk density (g cm^{-3}), field capacity (cm^3 cm^{-3}), wilting point water content (cm^3*cm^{-3}), and organic carbon content (cm^3 cm^{-3}). The annual land use maps from 2005 to 2015 were collected from the USDA-NASS Cropland Data Layer (USDA, 2019). Winter wheat and pasture were the most predominant crops in WCW. All the maps came in raster format with 30 x 30 m resolution which were then processed to a 120-m pixel resolution by taking the average soil properties in the 30-m cells comprising a 120-m cell.

Managing practices and fertilize application. For each agricultural land management practice, the planting date, harvest date, crop emergence date, and maturation date were included in the simulations to represent the growth cycle of crops. The land management data includes the time for cropping operations in the watershed such as the dates of planting, fertilizer application, emergence, maturation, and harvest. The timings for crop operations were adopted from the Agriculture Handbook No. 628 Usual Planting and Harvesting Dates for U.S. Field Crops (USDA, 1997). It should be noted however, that these dates were generated based on collected information from farmers in every state. They did not include the consideration of actual weather and field workability conditions. The fertilizer application data of the major crops in the land use map from National Land Cover Database (NLCD) (USGS, 2019a) was referenced from the Oklahoma Soil Fertility Handbook (Zhang and Raun, 2006), National Range and Pasture

Handbook (NRCS, 2003), and Oklahoma Forage and Pasture Fertility Guide (Arnall et al., 2011). The PRZM used these dates to estimate crop dynamics such as height, root depth, and canopy leaf area at each growing season. The fertilizer application inputs in PRZM requires the time, amount, and application method. To conceptualize the agricultural activities of the baseline scenario in PRZM, the following assumptions were made:

(1) Fertilizer was applied twice a year in both spring and fall in the baseline model;
(2) The N fixing crop decreases the amount of N fertilizer application for the other crop by 20 kg ha-1 in that year for double crops in one year (NRCS, 2003; Olson and Kurtz, 1982);
(3) For all the crops in the region, the planting day in the simulation is the middle day of the most active planting period and the harvest day in the simulation is the middle day of the most active harvest period (USDA, 1997).

Climate. The climate data used from 2006 to 2015 included daily rainfall time series, monthly average solar radiation, and monthly average temperature time series from five stations (Figure 1.1c). The daily rainfall time series was obtained from the USDA- Agricultural Research Service (ARS) Micronet Network for the five stations (Figure 1.1c) (Guzman et al., 2014; Starks et al., 2014). The monthly average solar fluxes were collected from the U.S. Solar Radiation Resource Map and daily maximum and minimum temperature time series were downloaded from National Centers for Environmental Information of National Oceanic and Atmospheric Administration (NOAA).

Streamflow and Nitrogen concentration. Daily streamflow and *N* load were needed to calibrate the historic baseline model. Daily streamflow was collected from the U.S. Geological Survey (USGS) National Water Information System database at the station of Willow Creek near Albert in Oklahoma (USGS 07325860) (Figure 1.1c) from 2006 to 2015. Total *N* in stream (g day^{-1})

was also available from the same source at irregular intervals from 2006 to 2012 (Moriasi et al., 2014).

Model calibration

Streamflow calibration. The simulated daily surface runoff was calibrated to the observed daily surface runoff. Among the PRZM parameters that were used in the calibration were the curve numbers, minimum depth of which evaporation is extracted, pan factor, and snowmelt factor. These parameters were adjusted to satisfy the following objective functions: (1) the cumulative simulated surface runoff matched the cumulative observed surface runoff from 2006 to 2015; and (2) the peaks in the simulated time series appeared when high surface runoff values in the observed time series were within a two-day interval. PRZM's performance in simulating the surface runoff was evaluated using the Mean Absolute Error (MAE), Percent Bias (PBIAS), Ratio of Standard Deviations (RSD), and Modified Index of Agreement (MD). The MAE and PBIAS measure the errors in the measured and simulated time series and water balance, respectively. The RSD evaluates the agreement in the distributions of the measured and simulated variables while MD is an overall "goodness of fit" indicator with 1 representing a perfect fit (Legates and McCabe, 1999).

Baseflow separation. PRZM lacks the fundamental hydrologic processes linked to the baseflow and is limited to surface runoff estimations. Therefore, it was necessary to separate the baseflow component from the measured flow to allow the comparison between measured and simulated flow and load. Baseflow separation was based on a digital filter using two-parameter Boughton algorithm; with $k = 0.99$ and $C = 0.066$ (Chapman, 1999) as follows:

$$Q_b(n) = \frac{k}{1+C} Q_b(n-1) + \frac{C}{1+C} Q(n)$$

(Eq.1.1)

Where:

$Q_b(n)$ is the base flow of day *n* ($m^3 s^{-1}$); $Q_b(n-1)$ is the base flow of day *n*-1 ($m^3 s^{-1}$); $Q(n)$ is the flow of day n ($m^3 s^{-1}$); k and C are the parameters of the equation.

N load calibration. The simulated daily *N* load was calibrated to the sampled total *N* load in the stream by adjusting *N* application rate, application efficiency, and spray drift. It should be noted that fertilizer application is not regulated in the United States and hence, no detailed monitored data of application rates was available. The application rates, were therefore, calibrated in this study with reference to the recommended amount suggested by agricultural handbooks. Since the observed *N* were only available at limited intervals during the 2006-2015 period, calibrating for *N* was performed to satisfy the following objective functions: (1) the simulated time series was in the same magnitude as the sampled total *N* load; and (2) peaks in the simulated time series appeared when high sampled load values were nearby. The simulated and observed *N* load were compared visually.

Scenario-based changes in WCW

Scenario-based changes that included land use changes, land management practices, and climate change were implemented in WCW to determine the combination of factors that can result in critical *N* load. The responses of WCW to these changes where compared with the outputs from the calibrated baseline model. Four different management factors were considered in this research including: (1) Crop rotation percentages; (2) *N* application rates; and (3) *N* application timings.

Crop rotation scenarios. The projected land use scenarios (2020 to 2070) were generated based on the land use maps from 2006 to 2015. Three different scenarios were considered with different percentages of two-year alfalfa crop rotation with the original crop. Alfalfa was chosen as the crop rotation plant every two years because it can improve the soil drainage situation and fix *N* during its growth due to its deep roots (PSA, 2017). In addition, alfalfa was regularly grown in this WCW based on the land use map from NLCD. To generate the land use practices scenarios, the land use was re-classified into three categories based on their historic land use from 2006 to 2015, and then the land management scenarios with different alfalfa crop rotation percentages were generated. Land use corresponding to open water and non-cultivated areas were left unchanged. For the baseline, the agricultural area was divided into two groups for each scenario. In the first group, a percent of cultivated area were set to allow crop rotation while the area corresponding to the second group remained unchanged. Percent of area splitting the two groups were set at 30 and 60% in a randomized approach and were changed every two years to simulate crop rotation where alfalfa would be cultivated instead of the original crop.

N application rate scenarios. The *N* application rate was simulated using three scenarios. In the first scenario (A0), we used the calibrated values obtained from the baseline model. In the second scenario the recommended application rates (A1) referenced by the Oklahoma Forage and Pasture Fertility Guide were used, while in the third scenario (A2), these recommended rates were doubled (Arnall et al., 2011). When crop rotation is implemented, no fertilizer is applied to alfalfa.

N application timing scenarios. *N* application timing scenarios were generated based on the number of applications of *N* fertilizer per year. In the baseline model, *N* fertilizer was applied twice a year (T0), before planting and after harvesting. A one-time application scheme, during

spring (TS), was adopted to determine the impacts of application timing on *N* load to decrease the *N* load during winter. In the one-time application scenario, the fertilizer application occurred in the middle of planting regardless of the projected weather conditions.

Projected climate. The climate data used from 2020 to 2070 included daily rainfall time series and daily average temperature time series while monthly average solar radiation was set to match the period from 2006 to 2015. The daily rainfall and temperature time series were obtained from the Coupled Model Intercomparison Project Phase 5 (CMIP5) multi-model dataset referenced in the Intergovernmental Panel on Climate Change Fifth Assessment Report (World Climate Research Programme, 2017). Data was downloaded from the Localized Constructed Analogs (LOCA) CMIP5 projections using the Representative Concentration Pathway 8.5 (RCP8.5) which represented the most serious global warming situation (Pierce et al., 2014). The LOCA-CMIP5 RCP8.5 ensemble is composed of 32 global circulation models from different global climate modeling groups.

Scenario combinations. Combinations of different land cover scenarios (Table 1.2) were simulated using the projected climate from 32 global circulation models under the LOCA ensemble. Twelve (12) land management scenarios were considered in which each model was simulated using 32 climate projections (from 2020 to 2070) for a total of 384 scenarios, each with 5,911 independent PRZM model runs. The changes in the seasonal and annual *N* load were evaluated across the watershed and in every cell to identify the combination of factors that can result in a critical *N* load. Note that the combinations of different land management schemes can result in unexpected response from the system. For instance, increasing the percentage of crop rotation can perhaps compensate for an increase in application rate. The scenarios were named according to the percentage of crop rotation (e.g., CR00, CR30, and CR60), application timing

(e.g., T0 and TS), and application amount (e.g., A0, A1, A2). For instance, CR00T0A1 represents a scenario with no crop rotation, fertilizer application occurring in spring and fall, and recommended amount of N fertilizer applied.

Table 1.1. Land management practices scenarios and notation used across the model simulations. CR = crop rotation (30% or 60%); T = application timing (spring or split between spring and fall); A = fertilizer application rate

No.	Scenario	Crop Rotation (%)	Fertilizer Application	
			Timing	Rate
1	CR00T0A0	0	Spring/Fall	Baseline value
2	CR30T0A0	30	Spring/Fall	Baseline value
3	CR60T0A0	60	Spring/Fall	Baseline value
4	CR00TSA0	0	Spring	Baseline value
5	CR30T0A1	30	Spring/Fall	Recommended amount
6	CR60T0A2	60	Spring/Fall	Twice recommended amount
7	CR30TSA0	30	Spring	Baseline value
8	CR30TSA1	30	Spring	Recommended amount
9	CR30TSA2	30	Spring	Twice recommended amount
10	CR60TSA0	60	Spring	Baseline value
11	CR60TSA1	60	Spring	Recommended amount
12	CR60TSA2	60	Spring	Twice recommended amount

Monthly N load analysis under different climate projections. To further analyze changes in *N* load under different climate projections from 2020 to 2070, monthly model outputs were used to

compute the probability of occurrence of *N* load, and were then classified in three categories: high, moderate, and low for each land management scenario. Probability categorization were defined as: (1) High: probability corresponding to the population of *N* load larger than or equal to the historic monthly baseline third quartile; (2) Moderate: probability corresponding to the population of *N* load larger than or equal to the historic monthly baseline first quartile and less than the third quartile set to represent 50% of the *N* load population ; (3) Low: probability corresponding of the population of *N* load less than the historic monthly baseline first quartile. The probability of monthly load (P_n) was computed as follows:

$$P_n = \frac{M_c}{M_T} \quad \text{(Eq.1.2)}$$

where M_c is the number of months with *N* load in the category; M_T is the total number of *N* load in the same month per climate projection equal to 50. A ternary plot was then constructed to show the changes in the *N* load probability under different climate projections on monthly basis per land management scenario.

Region-based analysis. Aside from agricultural practices, the fate of surface *N* also depends on the combination of factors including soil surface properties, land use, and climate. An analysis to identify cells that are "vulnerable" to high *N* load was performed. The cells that frequently generated the highest *N* load during heavy rainfall days from 2020 to 2070 were selected by the following methods:

(1) For every climate projection, the top 1% of the total simulation period with the highest rainfall, with threshold values ranging from 25 to 33 mm/day, was selected as the days with extreme rainfall events;

(2) Within the days with extreme rainfall events, all the cells were sorted based on their *N* load and the top 2.5% of the cells were selected as the most vulnerable cells under this climate

projection. As 24% of the world useable land has been degraded, 2.5% is selected representing the 10% most seriously degraded soil in the degraded soil (ELD, 2014);

(3) The frequency in which the most vulnerable cell appeared in each climate projection was computed using the baseline simulation. This frequency represents the ability of the cell to generate *N* via surface runoff and was referred to in this study as the Nitrogen Load Index (NLI). The cells with higher NLI tended to appear more frequently in the most vulnerable cells lists under different climate projections which suggested higher probability to generate more *N* load during heavy rainfall events.

To identify the factors and features that lead to higher NLI, a generalized linear model with Poisson regression was generated using the soil physical properties that are readily measurable in the field and the applied *N* fertilizer amount as independent variables and NLI as dependent variable. The Potential *N* Load Index (PNLI) of each cell in WCW was then calculated to evaluate the ability of generating *N* during extreme rainfall events as follows:

$$PNLI = \alpha(BD) + \beta(OM) + \gamma(FC) + \delta(WPC) \quad \text{(Eq. 1.3)}$$

where:

$PNLI$ is the Potential Nitrogen Load Index of the region (dimensionless), BD is the bulk density of the soil surface layer (g/cm^3), OM is the organic matter mass percentage in the soil surface layer (%), FC is the volumetric field water capacity of the soil surface layer (%), WPC is the volumetric wilting point water capacity of the soil surface layer (%), and α, β, γ, and δ are the regression parameters. Cells with larger PNLI tended to generate more *N* load via surface runoff

during days with heavy rainfall while cells with smaller PNLI tended to keep more *N* from being washed away by heavy rainfall.

Results and Discussion

Model calibration

The performance of PRZM to simulate the responds of WCW was evaluated by comparing the simulated and observed streamflow and *N* load. The model was calibrated by changing the surface runoff and *N* parameters where the streamflow calibration preceded the *N* load calibration.

The simulated and measured cumulative flow at the end of the simulation period (2006-2016) was 188 and 189 cm, respectively (Figure 1.2a). The modeling framework was able to represent the general behavior of streamflow observations with MAE of 0.06 and PBIAS of -0.60% and thus, it was assumed that it also represented the water circulation in this watershed. Note that there were no additional observations from other hydrological subsystems (e.g., groundwater, near surface) to validate the modeling framework. The RSD between the observed and simulated time series was 0.71 indicating a good match between the distributions of the two time series. Overall, the agreement between the simulated and observed surface runoff was reasonable (MD = 0.63).

The daily observed and simulated total *N* load both fell in the same order of magnitude (Figure 1.2b) which was one of the objective functions that we originally aimed for. The simulated and measured peaks were also observed to occur not more than 1 day apart. Since the observed *N* was not a continuous time series but grab samples instead, the one-to-one comparison of the observed and simulated time series was not possible. Also, the discrepancies brought about by incorporating the baseflow, which was estimated using the Boughton algorithm, in computing

the simulated total *N* load added another layer of uncertainty to the calibration process. The fact that PRZM only computes surface processes while measured variables include the contribution of both the surface and the baseflow (streamflow and *N* concentration) prevented the computation of proper metrics to quantify the model performance. Hence, the goodness-of-fit of the model was based on visual evaluation and an objective function that the simulated and observed *N* load should fall within the same order of magnitude.

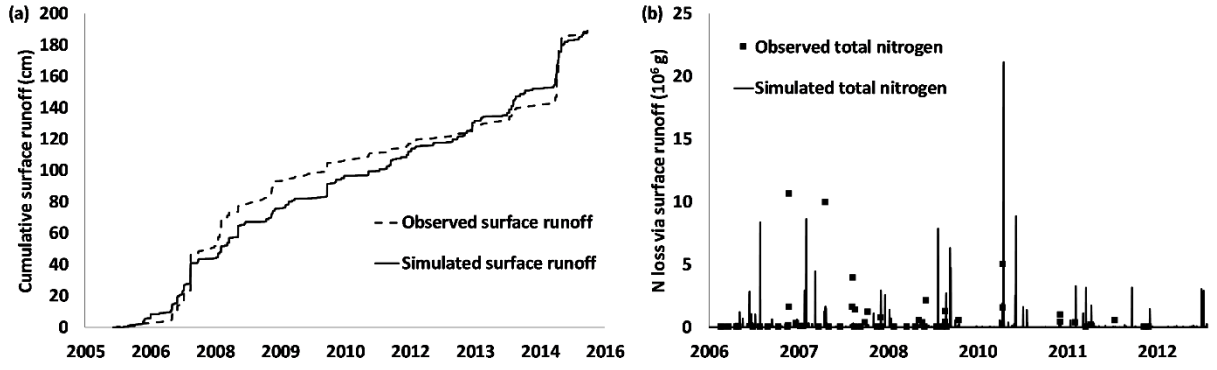

Figure 1.2. (a) Daily simulated and observed cumulative surface runoff; (b) Comparison between simulated *N* load and measured N from grab samples (i.e., instantaneous measurements of *N* taken at specific times).

Scenario-based simulations

Different combinations of land management scenarios were simulated to assess their corresponding impacts on *N* load under 32 climate projections from 2020 to 2070 (Figure 1.3, 1.4, 1.5). The probabilities of high, moderate, and low *N* load of the different scenario combinations were plotted in a ternary plot along with the historic baseline scenario for probability analysis (Figure 1.3, 1.4, 1.5).

Historic baseline in ternary plots. As the load used to determine the high and low *N* load were the top 25% and 75% of the historic values, respectively, the historic baseline points of all the 12 months are located at the point (P_{high}, P_{mid}, P_{low}) = (0.25, 0.5, 0.25) in the ternary plot. The unchanged location of the historic baseline points, indicated by a black square (e.g. Figure 1.3),

provided a visual analysis of expected changes in the occurrence of *N* load compared to the baseline under future scenarios. In the plot, the land management scenarios with more points in the upper vertex were expected to generate less high *N* load events compared to those in the lower left vertex. Therefore, the upper tip of the ternary graph, where $P_{high} = 0$ and $P_{low} = 1$, is the most sought-after condition. The plots can also be used to analyze the monthly *N* load behavior between different months.

Effects of projected climate

The projected annual mean rainfall from 2020 to 2070 is expected to increase on average by approximately 17% compared to the baseline rainfall from 2006 to 2015. Yet, the annual mean *N* load of scenario CR00T0A0, which was the projection of the historic baseline from 2020 to 2070, remained the same as the historic baseline from 2006 to 2015. Furthermore, the peak monthly *N* load was observed to occur one month earlier in the projected scenario compared to the baseline which can be due to the shift in the rainfall peak from June in the historic to May in the projected climate. However, the maximum monthly *N* load increased by approximately 43% compared to the historic baseline mean and this percentage rose to 1000% in January, which suggested that the monthly *N* load can reach a very high level under some climate projections. The probability analysis showed that significant changes in monthly *N* load probability distribution may take place from 2020 to 2070 (Figure 1.3a). The ternary plot for the projected baseline scenario, CR00T0A0 (Figure 1.3a) showed that high monthly load from March to May and from November to February were expected to happen more frequently compared to the historic baseline ($P_{high} > 0.25$). In fact, the occurrence of high *N* load was expected to be more than 75% for these months from 2020 to 2070. Meanwhile, the frequency of high monthly *N* load from June to October were expected to decrease from 2020 to 2070. The possible reasons for

these changes in the probability distribution of the monthly load from 2020 to 2070 included: (1) The peak rainfall shift from June to May in the future climate projections was expected to generate more surface runoff in May; (2) Climate changes resulted in generating more and heavier rainfall events which increased the frequency of high *N* load months in the future; and (3) The plants were expected to have more canopy past June resulting in more interception and less surface runoff.

Land management scenarios

Among the 12 land management scenarios simulated in this research, four of them were intended to reduce *N* load. These were 30% and 60% crop rotation combined with single fertilizer application or double fertilizer applications (Figure 1.4b to 1.4e). Another four scenarios (Figure 1.5b to 1.5e) were intended to analyze the tradeoffs between higher economic benefits and environmental welfare. These scenarios combined 30% and 60% crop rotation with increased application rates to determine if the effects of crop rotation can offset the impacts of increased *N* concentration from fertilizer.

Single application: The impacts of the application timing were evaluated using scenarios CR00T0A0 and CR00TSA0 through the monthly mean *N* load and the probability distribution among high, moderate, and low-level *N* load. Based on the results, the annual *N* load increased by 4% when the land management practice changed from spring-fall application (T0) to spring application (TS). Specifically, the monthly *N* load increased in May, June, July, and August (Figure 1.3c) in response to a full fertilizer application rate as opposed to a split load in spring-fall application. However, the probability analysis showed that the occurrence of high *N* load events (P_{high}) has decreased apart from May, June, and July, although P_{high} for June and July is still below the historic baseline. Results suggested that spring application was capable of

decreasing *N* load in most of the year at the cost of larger probability of high *N* load occurrences from May to July. However, research also showed that spring-fall application practice was expected to be more efficient since smaller amounts are timed to match major crop uptake periods (Edwards et al., 2006; Sowers et al., 1994).

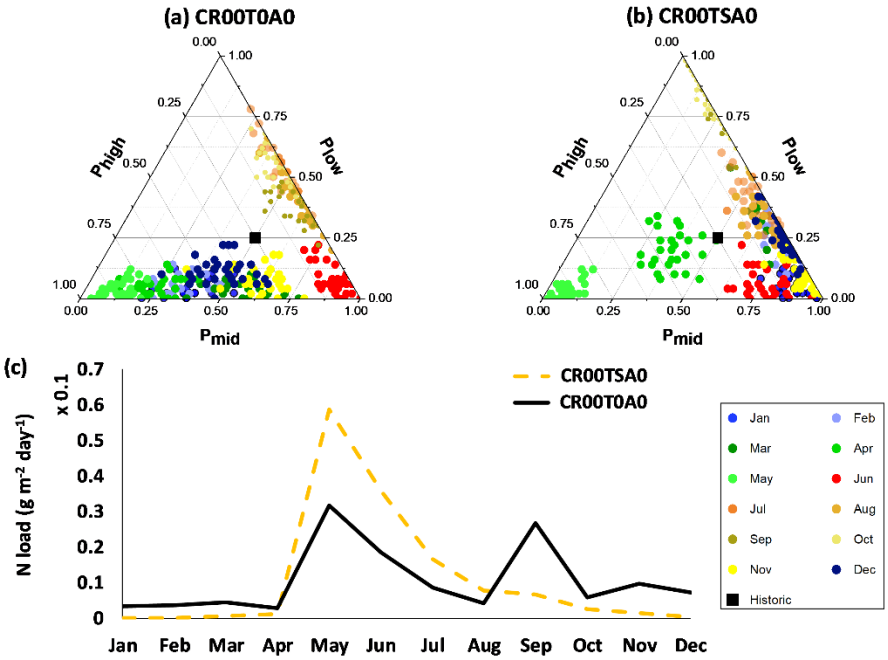

Figure 1.3. Monthly N load probability distribution ternary plots of the scenarios with (a) spring-fall applications and (b) spring applications, and (c) monthly mean N load from 2020 to 2070.

Crop rotation in split application: The impacts of crop rotation were evaluated using scenarios with different percentages of crop rotation cover (alfalfa) combined with spring-fall fertilizer application (T0). Scenarios CR30T0A0 and CR60T0A0 are examples of crop rotation variation in the watershed with fertilizer application in spring and fall. Overall, increasing the area where crop rotation was implemented in the watershed decreased *N* load since less *N* was applied on the soil compared with the scenario CR00T0A0 during the simulation period (Figure 1.4f). However, no notable differences were observed in the probability of occurrence of high *N* load (P_{high}) with these scenarios (Figure 1.4b and 1.4c) compared with the CR00T0A0 scenario

(Figure 1.4a) for months with high P_{high} (P_{high} > 75%). Additionally, unexpected increase in the monthly mean *N* load in August and October was observed in these scenarios compared with the CR00T0A0 from 2020 to 2070. This increase in *N* load in surface runoff was associated with the low canopy interception depth of alfalfa which was usually harvested every 35-49 days leaving the soil with less cover. Smaller canopy interception of rainfall was expected to generate higher surface runoff because PRZM simulated precipitation reaching the soil surface by subtracting plant interception first from the total precipitation. Smaller interception would result in more precipitation available for surface runoff. As curve number remained the same in the simulation, more precipitation reaching the soil surface would result in more surface runoff. In summary, increasing the coverage of crop rotation practice was expected to lower the *N* load but at the cost of increasing the occurrence of high *N* load events (P_{high}) in August and October.

Crop rotation and single application*:* The combined impacts of crop rotation and single application land management practice were evaluated using different percentages of crop rotation cover with annual spring application. Scenarios CR30TSA0 and CR60TSA0 are examples of crop rotation variation under single application in the watershed. Overall, the annual mean *N* load remained the same as that in CR00T0A0 during the simulation period. However, a significant increase in April and May *N* load was observed while the rest of the months posed decreases in *N* load (Figure 1.4f). This increase in April and May was because the *N* fertilizer application in spring doubled resulting in high *N* concentration in the soil surface in the months of April and May. After two months of plants absorption, leaching, and surface runoff, the *N* concentration in the soil surface was expected to drop which decreased the *N* load from surface runoff in the rest of the year. However, the probability analysis showed greater potential of single application in reducing the occurrence of high *N* load events (P_{high} < 0.75). In fact, only

four climate projections in June and 2 projections in January were expected to generate high *N* load more frequently than historic baseline by implementing 30% area of crop rotation (Figure 1.4d and 1.4e). If 60% of the area is converted to crop rotation, P_{high} of all the months besides April and May reduced to around 10% which meant that the probabilities of high *N* monthly load dropped to half of the baseline (Figure 1.4d and 1.4e). These results suggested that the *N* high monthly load appeared much less frequently from June to March by applying both single application and crop rotation practice.

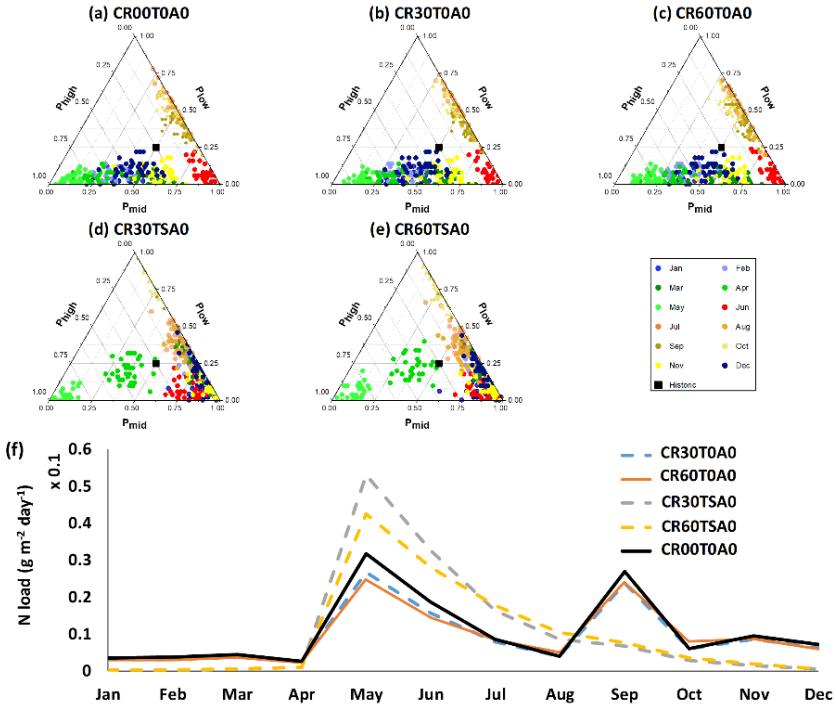

Figure 1.4. Monthly N load probability distribution ternary plots of the scenarios with different areas of crop rotation and (a, b, and c) spring and (d and e) spring-fall application under the baseline fertilizer application rate, and (f) their monthly mean N load from 2020 to 2070.

Increase in application rates. The monthly *N* load in surface runoff of scenarios CR30T0A1 and CR60T0A2 were compared with the scenario CR00T0A0 to determine if larger crop rotation area could reduce the *N* load even when the application rate was increased. The calibrated

application rates (A0) for different crops in the baseline model are shown in Figure 1.2 together with the rates recommended (A1) by the Oklahoma Forage and Pasture Fertility Guide (Arnall et al., 2011). Scenario CR30T0A1 combined the effects of 30% crop rotation and the recommended amount of fertilizer while CR60T0A2 determines the tradeoffs between increasing the fertilizer amount to twice the recommended and implementing higher crop rotation coverage. In both scenarios, the fertilizer was applied in fall and spring. Based on the results, a notable increase in the mean *N* load was observed in scenarios CR60T0A2 and CR30T0A1 compared with the baseline scenario. Furthermore, comparison of the monthly peak values indicated that the expected monthly peak load could increase to up to 680% of baseline in CR60T0A2 and 320% in CR30T0A1 (Figure 1.5f). Also, the frequency of occurrence of high *N* load events increased when the application rate increased regardless of the increase in crop rotation coverage. Comparison between the ternary plots of these scenarios and CR00T0A0 (Figure 1.5a to 1.5c) showed that the dots started moving towards the left vertex of the triangle when the application rate was increased.

The impacts of spring application, increased application rate, and crop rotation were determined in scenarios CR30TSA1 and CR60TSA2 (Figure 1.5d and 1.5e). Overall, the crop rotation and spring application were not expected to offset the negative environmental effects from the doubled *N* fertilizer application rate. The increase in *N* load was more than 800% from May to August which meant that the average *N* load level was expected to be kept at high level during summer (Figure 1.5f). However, crop rotation combined with spring application was expected to keep the *N* load the same as the historic baseline when the recommended rate of *N* fertilizer was applied during most of the year. Based on Figure 1.4d, the occurrence of high monthly *N* load was kept at the same level as historic in all the months expect April and May. In summary, our

results revealed that increasing crop rotation area combined with spring application was expected to cancel the negative effects of *N* fertilizer at recommended application rate. However, neither crop rotation nor spring-application was expected to lower the *N* load to the historic level.

Table 1.2. Calibrated and recommended N fertilizer application rates.

Crop type	Recommended application amount (kg/ha)	Baseline application amount (kg/ha)
Corn	101	51
Cotton	68	34
Sorghum	68	34
Winter Wheat	101	51
Peanuts	336	168
Rye	68	34
Oats	101	51
Grassland/Pasture	68	34

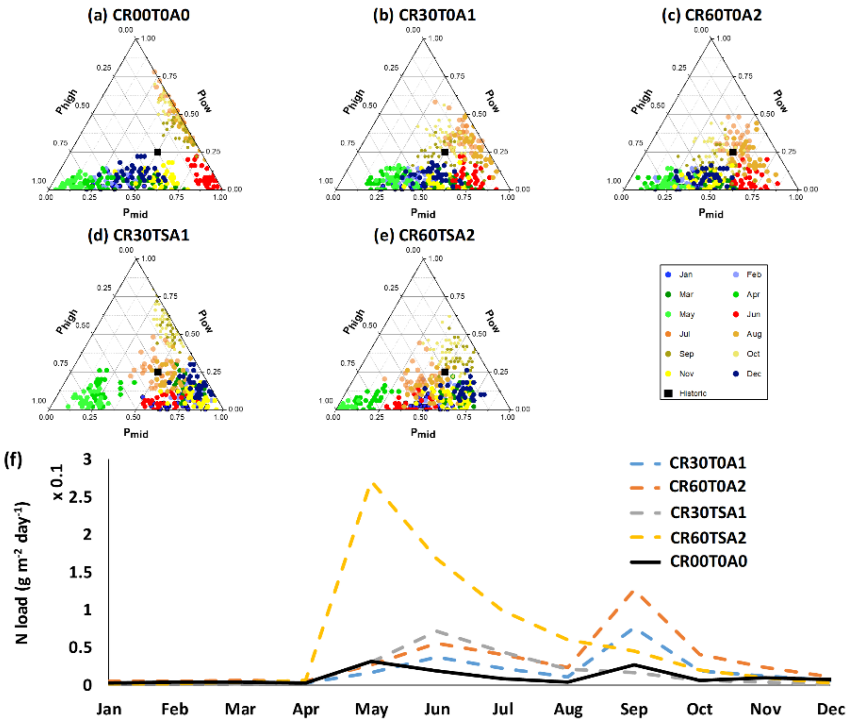

Figure 1.5. Monthly N load probability distribution ternary plots of the scenarios combining different areas of crop rotation with (a, b, and c) spring-fall or (d and e) spring application under the recommended or double the recommended amount of N fertilizer applied, and (f) their monthly mean N load from 2020 to 2070.

Region-based analysis

The Nitrogen Load Index (NLI) of every agricultural region was generated to determine the general behavior of the region in generating *N* load during a storm event. Based on the generalized linear model with Poisson distribution, we found that a soil surface with higher bulk density, organic matter, and field water capacity was expected to lose less *N* load during heavy rainfall events. On the other hand, a soil surface with higher wilting point water capacity and higher application *N* rate was expected to generate more *N* load during heavy rainfall events. To eliminate the effects of different *N* application rates on NLI, the PNLI of every agricultural region in WCW watershed was calculated to evaluate the ability of losing *N* during extreme rainfall events based on the regression model of NLI. After fitting a Poisson distribution to the

data, the regression parameters α, β, γ, and δ were found to be -47, -0.464, -3.37, and 4.18, respectively, with $p << 0.01$. The resulting equation for PNLI was:

$$PNLI = -47 * BD - 0.464 * OM - 3.37 * FC + 4.18 * WPC \quad \text{(Eq. 1.4)}$$

Customized land management

The *N* load from the watershed during days with heavy rainfall was expected to decrease if we re-assign the land uses based on their PNLI (Figure 1.6b). To reduce the *N* load without applying less *N* in the field, the agricultural cells in baseline land use from 2020 to 2070 were assigned new land use scenarios to specifically target what the cells require to lower the *N* load. Since the application rate was found to be the dominant factor that controls the *N* load, the land use scenarios with higher mean annual *N* fertilizer application rate were assigned to the cells with lower PNLIs. The new scenario was then simulated under 32 climates from 2020 to 2070 to determine the effects of the redistribution of land use.

By applying the *N* fertilizer based on the PNLI of the soil cells, the monthly *N* maximum value decreased by 13.4% and the annually mean *N* load decreased by 6.1% (Figure 1.6b). In addition, the most critical month also changed from September to May. As discussed above, lower and earlier *N* load peaks were expected to cause less environmental problems to the watershed ecosystems due to the lower water temperature. In addition, the occurrence of months with high *N* load and moderate *N* load also decreased from May to October which indicated that the target application management was expected to improve the *N* load behavior (Figure 1.6a). However, as only the *N* load in surface runoff was considered in changing land management practices, the effects of target application management on the economic benefits were unclear. It was assumed that increasing the application rate can increase the productivity of the system.

Customized field scale land management practices can be implemented following the methodology illustrated in this study. Identifying areas that are most vulnerable to surface runoff and *N* loss and targeting specific practices to mitigate this can result in a more sustainable farming system where productivity and environmental soundness are optimized. Due to the spatial variability of factors affecting transport processes, this approach is expected to result in a more efficient use of resources than when land management is implemented across an entire area.

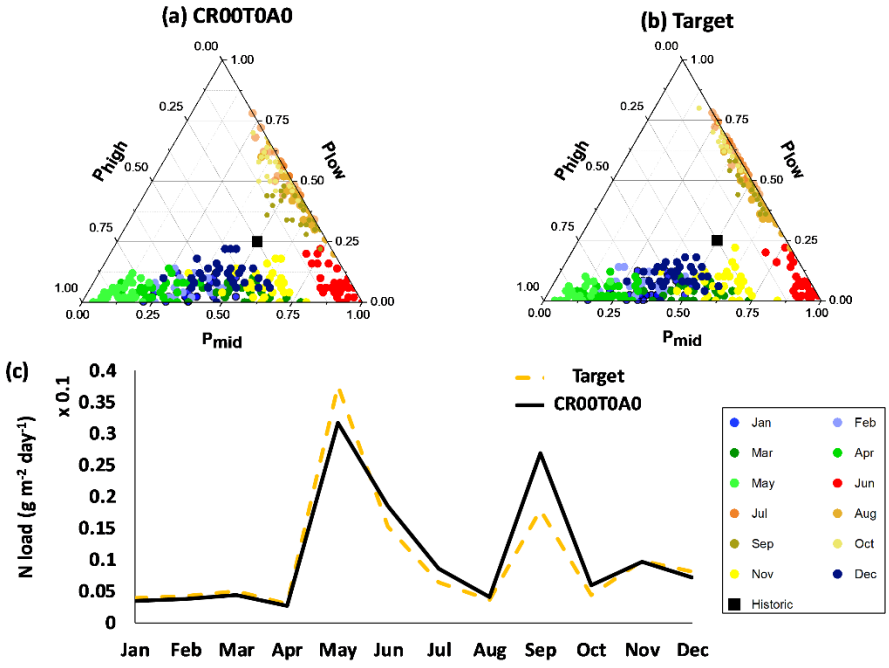

Figure 1.6. Monthly N load probability distribution ternary plots of (a) the projected baseline and (b) the target application management scenarios, and (c) monthly mean N load from 2020 to 2070.

Conclusions

This study evaluated the effects of different land management practices on *N* load in surface runoff under future climate projections at the filed scale level. The combinations of land management practices were also evaluated to determine those that can increase productivity with

minimal negative impacts on the environment. Moreover, this study developed a methodology to identify areas most vulnerable to generate *N* load in surface runoff and to target specific management to these areas. Based on our results, crop rotation practices lowered both the *N* load and the probability of high *N* load. Furthermore, when fertilizer is applied during spring instead of the split spring-fall application, crop rotation can cancel the negative effects of increasing the fertilizer rate to the recommended amount. Spring application reduced the negative effects in summer and fall from other land managements but at the risk of increased probability of generating high *N* load in April and May. Our results also confirmed that fertilizer application rate was the most critical factor in determining both the amount and the probability of high *N* load. To address this issue, the target application management approach could be implemented at the field scale to customize land management practices to reduce the amount and probability of high *N* load.

CHAPTER 2: MODELING FIELD SCALE NITROGEN NON-POINT SOURCE POLLUTION (NPS) FATE AND TRANSPORT: INFLUENCES FROM LAND MANAGEMENT PRACTICES AND CLIMATE[2]

Introduction

The use of nitrogen fertilizer marked the start of modern agriculture that boosted food production to help alleviate food shortages across the globe. It is suffice to say that the modern society was built on the solid base of agricultural production in which the 850% increase in global N fertilizer use during the last five decades (Lu and Tian, 2017) played a critical role. However, the massive use of N fertilizer has also brought severe environmental issues and critical stress to the agroecosystem due to the fact that over 25% of the total N applied was lost via leaching and surface runoff (Smil, 1999). The N transported from farmlands, about $4\ x\ 10^{13}$ g N annually, led to high N load in most of the rivers across the globe. Different environmental problems such as harmful algal bloom (HAB), decline in biodiversity, and unpleasant smell, were all related to excessive load of different types of N, including nitrate, nitrite, ammonia, and other types of organic N, in water bodies (Nakaji et al., 2001; Oenema and Roest, 1998; Timmons et al., 1973). To address these concerns, different mitigation strategies are being implemented globally. For example, N nonpoint source pollution was a critical part of the ongoing national environmental project, "The Gulf Hypoxia Action Plan" (Mississippi River/Gulf of Mexico Watershed Nutrient Task Force, 2008). In this project, the U.S. Environmental Protection Agency (EPA) has targeted a 45% decrease in nitrate N load in the Mississippi River basin which was also the long-term reduction goal of upstream states contributing to the basin (e.g. Illinois Nutrient Loss Reduction

[2] Hou, C., Chu, M. L., Botero-Acosta, A., & Guzman, J. A. (2021). Modeling field scale nitrogen non-point source pollution (NPS) fate and transport: Influences from land management practices and climate. Science of The Total Environment, 759, 143502.

Strategy) (Wilhite et al., 2015). The EPA also imposed regulatory limits for maximum contaminant level (MCL) of nitrate for drinking water to be 10 mg/L or 10 ppm (EPA, 2018). Nitrate N is the major nonpoint source (NSP) pollutant that can result in environmental problems such as HAB (Paerl, 1997) and contaminated drinking water which can lead to serious public health threats (Savino et al., 2002). Nitrate, which is relatively stable in the agroecosystem, can transform into other types of N NPS such as nitrite and ammonia that can cause other serious environmental problems such as fish kills and odorous water. Under some extreme anaerobic conditions, nitrate can be transformed into nitrite, which is toxic even at low concentration and can cause large scale of fish kill in the river. After nitrite is generated from nitrate, it can either decay into dinitrogen or transformed into ammonia N via denitrification. Ammonia N is considered safe to humans at low concentration but can still threaten the overall quality of water for domestic use. For instance, concentration of 1.5 mg/L of ammonia can be recognized by odor and at 35 mg/L by taste which aggravates the quality of drinking water (WHO, 2003). Moreover, ammonia N can also trigger algae bloom near the pollution sources (Domingues et al., 2011). Suffice it to say, different forms of N pollutants can result in different environmental problems and should be taken into consideration in the management practices aimed at addressing NPS pollution. Failure to do so might cause the inability to detect the possible environmental problems caused by the other forms of N. For example, a research by Kelso et al., (1997) found that nitrite could be accumulated via nitrate reduction under anaerobic conditions in the Northern Ireland rivers leading to low dissolved oxygen (DO) in water and high possibility of algal bloom (Kelso et al., 1997). Nitrous oxide (N_2O), which can be generated via denitrification process from nitrate in the rivers in both urban and suburban area, has proven to be one type of the greenhouse gases and harmful to the ozone (Beaulieu et al., 2011). As a result, agricultural land

management practices should be evaluated not only on their ability in reducing N load but also by better understanding the changes within N cycle transformations.

To address these problems, land management practices that are specific to tackle the different N components should be implemented. This, however, requires a thorough understanding of the N transformation and dynamics within the agro-ecosystem. The objective of this research was to better understand the different types of N NPS behavior in a highly cultivated watershed under wet and dry future climate projections when implementing different land management practices. Particularly, this paper was aimed at determining the fate and transport of nitrate, nitrite, and ammonia under future climate projections by adapting the recommended land management practices that are supposed to reduce nitrate N in surface water to state government target. In addition, the nitrate N concentrations in unsaturated zone and saturated zone were also analyzed to understand the possible impacts on crop growth and groundwater quality. To accomplish these objectives, a fully-distributed physical-based hydrologic model, MIKE SHE, and a hydrodynamic river model, MIKE 11, were coupled with ECO-Lab to simulate the fate and transport of different forms of N in the agro-ecosystem in the Upper Sangamon River Basin (USRB), a highly cultivated watershed in central Illinois.

Methods

Study Area

The USRB (Figure 2.1) was used to develop the MIKE SHE and MIKE 11 models combined with ECO-lab to simulate the fate and transport of the different components of N across the watershed. Located in central Illinois and covering an area of approximately 2400 km^2, the USRB is a highly cultivated watershed (84% agriculture) in which mainly soybean and corn are grown (NRCS, 2016). Lake Decatur, the outlet of the USRB, is used as the main water source

for both the City of Decatur and the Village of Mt. Zion with a total population of nearly 80,000 (United States Census Bureau, 2019). The nutrient load from fertilizer applications in the croplands has threatened the drinking water quality in the lake and has contributed to other environmental problems in the waterways. Research showed that the annual nitrate N concentration has increased by 0.087 mg/L each year at Monticello from 1993 to 2018 and the N concentration in the USRB has exceeded the drinking water standard of 10 mg/L since 1980 (Keefer et al., 2010). In addition, the sediments from the USRB basin also decreased the capacity of Lake Decatur by 33% from 1922 to 1983 (Keefer et al., 2010).

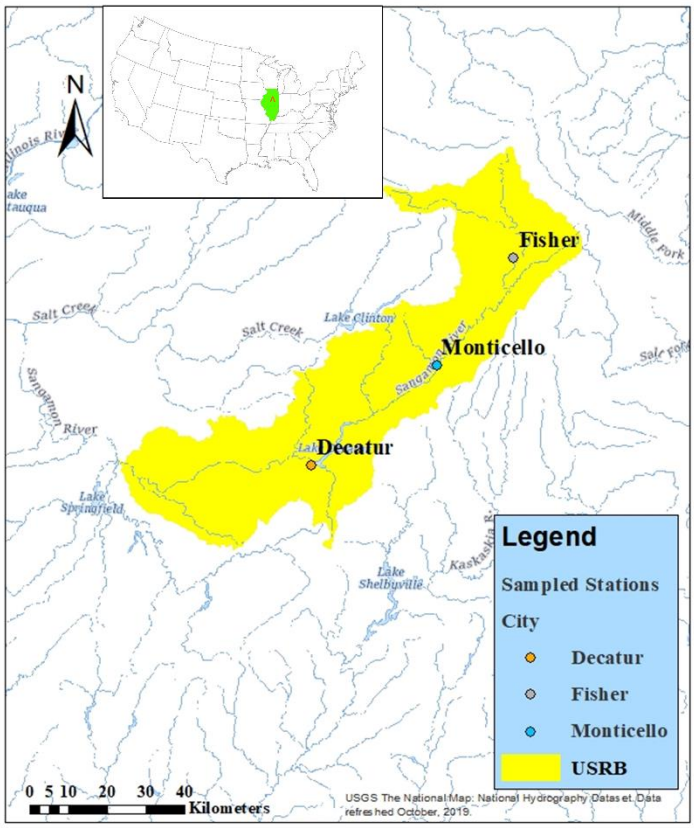

Figure 2.1. The Upper Sangamon River Basin and its streamflow stations at Decatur (Decatur, Fisher (Fisher), and Monticello (Monticello) in central Illinois (USGS, 2020) and Illinois (shaded area) in the United States.

To address the environmental problems in the USRB, efforts have been made including a dredging project which aimed to recover the capacity of Lake Decatur and the implementation of management practices aimed at reducing N load in conjunction with the Illinois Nutrient Loss Reduction Strategy (ILEPA, 2019).

Model set-up and parameterization

The MIKE ECO-lab model was used to simulate the transformation of N from applied fertilizer based on the hydrologic model developed by Botero-Acosta et al. (2018) where MIKE SHE and MIKE 11 were used to simulate the water movement and contaminant transport across the USRB and the rivers, respectively (Alejandra Botero-Acosta et al., 2018). MIKE SHE, which is a deterministic, physically-based, fully distributed model, was used to simulate the water and contaminant movements on the surface, the vadose zone, and the groundwater. It is a fully coupled hydrologic model that seamlessly integrates the surface and subsurface allowing feedback and feedforward mechanisms to occur. MIKE 11, which is a hydrodynamic 1-D river model, was used to simulate water and contaminant movement in the river channel (DHI, 2017b). Both models were set up using the measured and calibrated parameters in Botero-Acosta et al., (2018) across USRB discretized into 300-m grids. The models were then simulated from 1978 to 2015 for the baseline and from 2020 to 2050 for future climate projections with a daily time step.

The MIKE SHE/MIKE 11 model structure and data requirements can be compartmentalized into five coupled systems (Figure 2.2): the atmosphere, the surface, the unsaturated zone, and the saturated zone developed in MIKE SHE and the river and lake system developed in MIKE 11. Each compartment requires model inputs that are measurable from the field (Figure 2.2). The fluxes in each compartment was computed using physically-based equations such as the 2D

Richards' equation for the unsaturated zone and the 3D Darcy flow equation for the saturated zone. Subsurface tile drainage system is commonly installed in Central Illinois like the USRB. Approximately 59% of USRB was simulated with subsurface tile drain and over 95% of the nitrate in the streamflow in USRB was found to come from drain flow (A. Botero-Acosta et al., 2019). In the MIKE SHE model, the drainage flow was calculated as the product of the drain time constant and the water table height above the drains to simulate the effects of the drainage system draining excessive water from the unsaturated zone. In this research, the drainage system was installed uniformly 1 m below the soil surface with a drain time constant of $3 \times 10^{-7} m^2/s$. The overland flow was determined by solving the flow diffusive wave equation with the two-dimensional finite difference method. In MIKE 11, the flow was calculated by 1D hydrodynamic equation and kinematic routing.

Water quality is simulated in MIKE SHE and MIKE 11 as the fate and transport of a generic species, for instance, N. The transformation of N into nitrate N, ammonia N, and nitrite N need to be defined for the compartments where the processes take place, for example, the rivers. For the USRB, the main source of N is crop production and hence, for cells planted with corn, N was applied on the soil surface as nitrate N while ammonia N and nitrite N are transformed from nitrate N via N cycle. In addition to the nitrogen input to the model from fertilizer, the point sources load of N were also included in this model because the USRB had the most point loads of nitrogen in Illinois (ILEPA, 2019). Based on the results from Enforcement and Compliance History Online by EPA, point sources of nitrate N were added to MIKE 11 as boundary conditions at the closet river branch (A. Botero-Acosta et al., 2019; USEPA, 2019). The detailed model parameterization and set-up of MIKE SHE and MIKE 11 for the USRB can be found in Botero-Acosta et al., 2018 and Botero-Acosta et al., 2019.

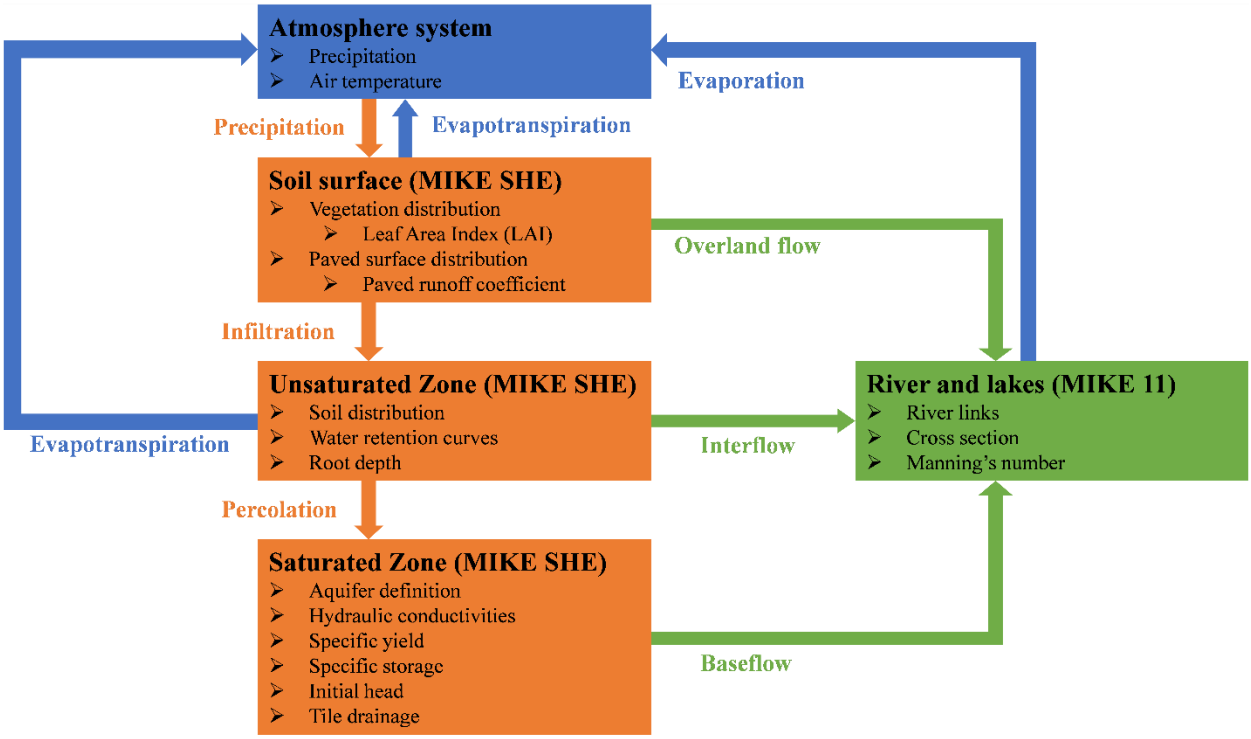

Figure 2.2. MIKE SHE/MIKE11 model structure and input data requirements. The boxes represented the different components of the system and arrows the main fluxes.

ECO-lab model set-up for N

The ECO-Lab model is an ecological model for water quality in aquatic ecosystems that can be customized for different systems, processes, and contaminants. The ECO-Lab model included both state variables standing for different components in the ecosystems and processes including chemical, biological, and ecological processes. It uses the inputs in MIKE SHE for the water movement in the overland, the unsaturated zone, and saturated zones, and the water movement in the river from MIKE 11. In addition, the ECO-Lab model also used soil temperature from MIKE SHE models and water temperature from MIKE 11 model.

Three ECO-lab models were set up representing the N cycles in the saturated zone, unsaturated zone, and surface water system. In each of the model, nitrate N, nitrite N, and ammonia N

(including ammonium N) were included as state variables and decay, nitrification, and denitrification processes were simulated (Figure 2.3). The decay processes included the processes that transformed the state variables into other forms of N that is out of the system. The nitrification processes included the processes that transformed ammonia into nitrite and further to nitrate while the denitrification processes included the processes that transformed nitrate back into nitrite and further to ammonia via biological and chemical reactions.

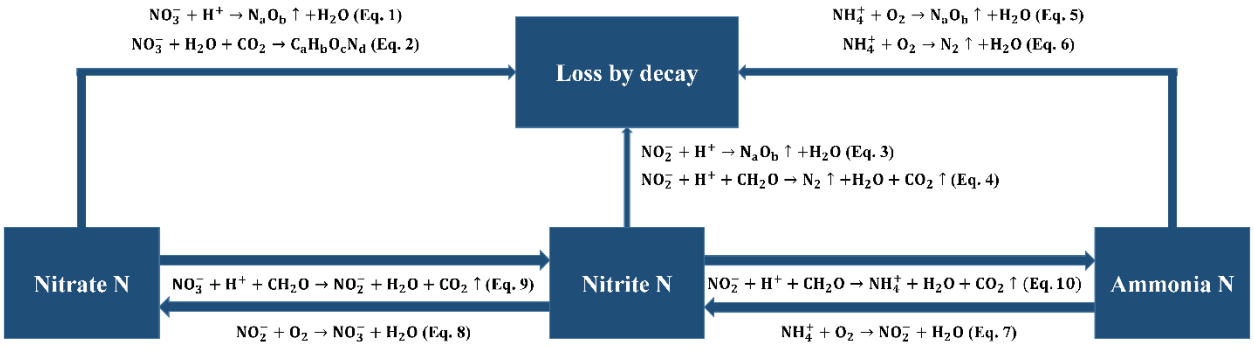

Figure 2.3. N cycle simulated in the ECO-Lab model and the chemical equations represented.

Conceptualization of processes in ECO-lab

A first-order exponential decay function was used to represent the N transformations represented in Figure 2.3. The governing equation used to represent all the bio-chemical processes in each hydrologic compartment (i.e., surface water, unsaturated zone, and saturated zone) was:

$In\frac{C_0}{C} = kt$ (Eq. 2.11)

where C_0 is the state variable concentration at the start of each time step; C is the state variable concentration at the end of each time step; t is the length of each time step; k is the estimated decay rate for different state variables at temperature T computed as follows:

$k = k_{20}\theta^{T-20}$ (Eq. 2.12)

where k_{20} is the estimated reaction rate at 20℃ (293.15 K); θ is the estimated temperature correction factor; T is the water temperature for ECO-Lab built for surface water and soil temperature for ECO-Lab built for unsaturated zone and saturated zone.

The ECO-lab model in the different hydrologic compartments were a collection of processes in the whole N cycle with different reaction constants changed based on its physical conditions and calibrated based on the measurements from two stations (Fisher and Monticello) using grab samples collected from 1991 to 2017 (USGS, 2019b).

N cycle in surface water

N cycles in surface water changed based on the water depth. As sunlight and DO were higher near the water surface due to air exchange and photosynthesis from phytoplankton, the reaction rates of nitrification processes (Eq. 2.7 & Eq. 2.8) and nitrate decay due to process of assimilation from phytoplankton (Eq. 2.2) were accelerated and denitrification processes (Eq. 2.9 & Eq. 2.10) were limited. Deeper into the water profile, the DO decreased which limited the nitrification processes (Eq. 2.7 & Eq. 2.8) and accelerated the denitrification processes (Eq. 2.9 & Eq. 2.10).

The N cycle which was set up in the ECO-lab model in this research represented the general N cycle in surface water as a whole system. As a result, the nitrification processes (Eq. 2.7 & Eq. 2.8) in surface water were faster than the processes in the soil because of the DO released via the photosynthesis processes from phytoplankton and higher air exchange rate between flowing water surface and the atmosphere.

N cycle in the unsaturated zone

All the processes in the N cycle were expected to take place in the unsaturated zone but the rates of the processes changed based on the availability of oxygen (air), water, temperature, pH, and

organic matter. As a result, N cycle in unsaturated zone included all the possible transformation processes (Eq. 2.1 to 2.10) and it was highly related to the fertilizer efficiency. Higher nitrate N and ammonia N concentration that persevered in the soil profile means higher fertilizer efficiency while higher nitrite N concentration in the soil profile can decrease crop production and harm crop heath.

In this model, only the soil temperature was taken into consideration due to the lack of data to represent the other variables. Furthermore, the nitrate decay rate was much higher in the unsaturated zone because the nitrate absorption by crops was also included in the decay process.

N cycle in saturated zone

The saturated zone is characterized by the low amount of available DO and slow water movement which resulted in lower reaction rates for all the processes included in the ECO-lab model. However, as the conditions became extremely anaerobic in the saturated zone, the reaction constants of Eq. 2.10 and Eq. 2.9 were expected to be higher than the other reaction constant in this system.

ECO-Lab model calibration

The decay rates, *k*, representing Eq. 2.1 to 2.10 were determined through calibration by comparing the measured and the simulated nitrate N, nitrite N, and ammonia N at Fisher and Monticello.

The baseline model that simulated the fate and transport of N from 1981 to 2015 with three years of warm-up period from 1978 to 1981 was developed to reflect the impacts of the historic climate and land use in USRB. The baseline model was calibrated by changing the reaction parameters in Eq. 2.11 in the ECO-lab model, and the fertilizer application rates and application timings in MIKE SHE. The performance of the ECO-lab model to simulate the changes in nitrate

N, nitrite N, and ammonia N was evaluated by comparing the measured concentrations of N at the gauging stations in Fisher and Monticello, where measurements were more substantial, with the simulated N generated by the MIKE model ensemble from 01/01/1981 to 12/31/2015. The measured concentrations were collected using grab sampling method which were instantaneous measurements of water samples at a specific time at a given location. Due to the lack of continuous measurements, the calibration process was performed during different time periods selected based on the density and frequency of the grab samples. Four periods were used to evaluate the performance of Eco-lab in simulating the different components of the N cycle in USRB: Period 1 (04/21/1991-10/29/1991), period 2 (09/26/1996-09/22/1998), and period 3 (02/05/2001-09/25/2008) were selected at Monticello for nitrate N, nitrite N, and ammonia N and period 4 (12/19/1985-05/01/1997) at Fisher for nitrate N.

Land management practices scenarios

Cover crops and crop rotation have been used as nutrient management schemes to decrease the N load in water bodies, improve soil hydraulic conductivity, and boost agricultural production (X. Cheng et al., 2019; Dinnes et al., 2002; Karlen et al., 2006; Unger and Vigil, 1998; VanDyke et al., 1999). In the USRB, one of the most common crop rotation schemes was the corn-soybean rotation with a possible idle time for the soil to recover its nutrients (Karlen et al., 2006). In this study, the cover crop management practices were adapted based on the corn-soybean rotation (Table A.1) following the recommendations of the Midwest Cover Crops Council (Woodyard et al., 2019b, 2019a). The new scheme involved planting cover crop during the idle period in the corn-soybean rotation (Table A.1). This means that another crop was planted in the late fall and grown in the early spring before the seeding of next year crop. Specifically, the cells originally planted with corn in summer and fall (May to October) were planted with oats/radish in spring

(last year November to April) and cereal rye in winter (November to next year April). Similarly, cells originally planted with soybean in summer and fall (May to October) will be planted with cereal rye in spring (last year November to April) and oats/radish in winter (November to next year April).

To build the new land management scenario for crop rotation and cover crop in MIKE-SHE, the corresponding cover crops were added to the corn and soybean cells during winter and spring. The cells which were not corn or soybean remained the same from 2020 to 2050 as their land uses from 1978 to 2015. To represent the cover crop in MIKE SHE, the cover crop information (i.e., changes in the leaf area index, crop coefficient, and root depth) was added to that of corn or soybean. Similarly, the hydraulic conductivity of soil surface layer was also increased by 20% to represent the effect of cover crop roots in spring and early summer (Bodner et al., 2008).

Fertilizer application rates scenarios

To determine whether or not the nitrogen load reduction target in The Gulf Hypoxia Action Plan" (Mississippi River/Gulf of Mexico Watershed Nutrient Task Force, 2008) can be achieved through the ongoing land management schemes in USRB, different combinations of corn-soybean rotation, cover crop, application rates, and future climate were created as scenarios (Table A.2). In these scenarios, the application rates for all the crops were reduced by 50% to simulate the scenario if state government regulated the fertilizer application rate to meet the reduction goal in the project. Furthermore, cover crop scenarios were also implemented in combination with the reduced rates scenarios to simulate the combined effects on the N load.

Climate projections

The future climate projections used in this research were generated from the Coupled Model Intercomparison Project phase 5 (CMIP5) from the Working Group on Coupled Modelling

(WGCM) of the World Climate Research Programme's (WCRP) (World Climate Research Programme, 2017). The CMIP5 includes global circulation models (GCMs) from 20 modeling groups across the globe under different emission levels simulating climate projections for the future. Among the models under the highest emission condition in the project, the Representative Concentration Pathway (RCP) 8.5, the driest and wettest climate projections were identified based on the mean rainfall and daily temperature to simulate the possible range of future climate projections. The GFDL-CM3 model was identified to generate the highest mean rainfall which was used as the "wet" climate projection and GFDL-ESM 2M model was identified the lowest mean rainfall which was used as the "dry" climate projection, respectively (Alejandra Botero-Acosta et al., 2018).

Simulation of scenarios

The corn-soybean, cover crop, and reduced fertilizer application were simulated under the historic and projected climates in both wet and dry conditions which resulted in 12 scenarios (Table A.2). The *baseline* scenarios simulated the historic land use from 1978 to 2015 under historic climate *(baseline A)*, wet future climate *(baseline B)*, and dry future climate *(baseline C)*. In addition, to evaluate the effectiveness of government regulated fertilizer application rate, the *regulated* scenarios were the simulations of historic land use with 50% less fertilizer applied under historic climate *(regulated A)*, wet future climate *(regulated B)*, and dry future climate *(regulated C)*. Furthermore, to evaluate the effectiveness of adapting cover crop land management practice for corn and soybean, the *updated* scenarios simulated the impacts of the updates land management that combined crop rotation and cover crops under historic climate *(updated A)*, wet future climate *(updated B)*, and dry future climate *(updated C)*. The regulated

and updated scenarios were combined to constitute the *combined* scenarios under historic climate *(combined A)*, wet future climate *(combined B)*, and dry future climate *(combined C)*.

Baseline N model

The calibrated reaction constants that represented the transformation of the different components of N were shown in Table A.3. Generally, the calibrated *k* values were lower than the values measured in the laboratory as reported in the literature for the same transformations under ideal conditions. This was expected since factors such as pH, supply of reactant, DO concentration, and temperature were expected to differ in the fields (I. F. Cheng et al., 1997; Dinçer and Kargi, 2000; McLaren, 1976; Shah and Coulman, 1978). In addition, the rate constants were expected to be further decreased by the competitive effect from other bio-chemical reactions (Hockenbury and Grady, 1977; Verhagen et al., 1995). For example, the DO in surface water could be consumed by both bacteria and other oxygen needing reactions, which was expected to decrease the DO concentration available for nitrification (Eq. 2.7 and Eq. 2.8) and lead to the decrease in the nitrification reaction rate.

The fertilizer application rates of the different crops were also calibrated based on the sampled nitrate N, nitrite N, and ammonia N concentrations in the river. The typical N fertilizer used in USBR was ammonia or UAN, which were expected to transform into nitrate N in less than a week after application. As a result, N fertilizer in MIKE SHE was simulated as nitrate N applied either after harvesting or before seeding. The calibrated nitrate N application rate for corn was 285 kg/ha per year which was after harvesting from 1978 to 2008, 75% after harvesting and 25% before seeding from 2009 to 2011, and 60% after harvesting and 40% before seeding from 2012 to 2015 (A. Botero-Acosta et al., 2019; IPNI, 2020).

The performance of the MIKE model ensemble in simulating the fate and transport of nitrate N, nitrite N, and ammonia N was evaluated by comparing the measured and simulated N concentration at Fisher and Monticello. For nitrate N (Figure 2.4), the calibration results were evaluated by comparing the measured and simulated variables using scatter plots and daily time series. As nitrate N is relatively a stable chemical in the river system under normal conditions (less than 70℃), the grab samples were expected to represent the nitrate N level to some degree (Aminot and Kérouel, 1995). Furthermore, the irregular frequency of sampling prevented the use of model performance metrics for continuous measurements, for instance, the Nash-Sutcliffe Coefficient. As a result, the goodness-of-fit of the model was based on both visual evaluation of the time series as well as the coefficient of determination, R^2 (Figure 2.4). In addition, the simulated time series showed the same seasonal tendencies and fell within the same order of magnitude as the measured time series indicating a good fit of the model.

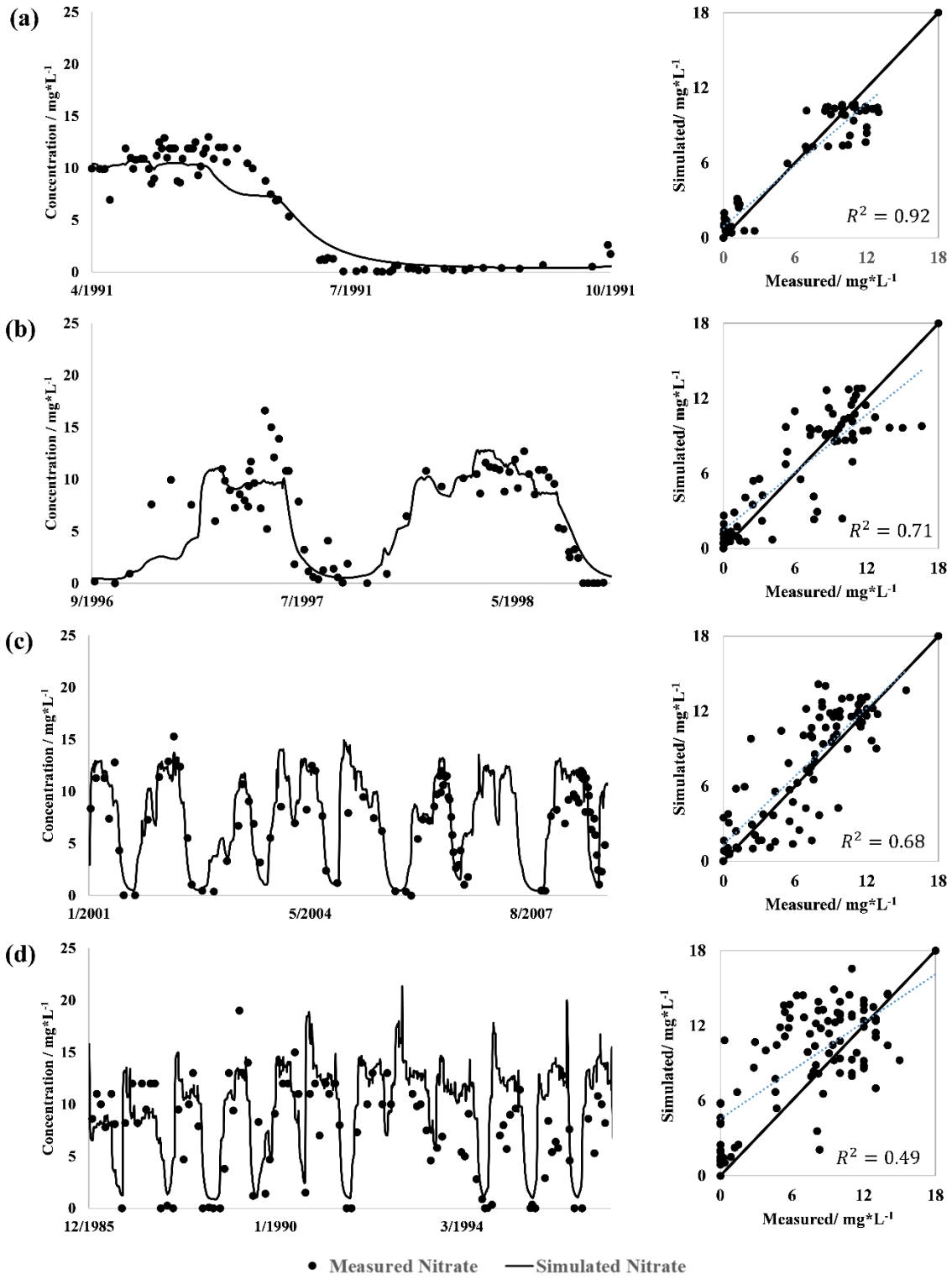

Figure 2.4. Observed and simulated nitrate N at four different periods and stations: (a) Period 1 at Monticello; (b) Period 2 at Monticello; (c) Period 3 at Monticello; and (d) Period 4 at Fisher.

For nitrite N (Figure A.1) and ammonia N (Figure A.2), only the comparison of the measured and simulated time series was plotted. Due to the instability of both nitrite N and ammonia N compared with nitrate, nitrite N could transform into other forms of N depending on the pH, DO, and COD of the water, while the ammonia N in the water could be released into the atmosphere due to its high volatility. The simulated values of nitrite and ammonia were unable to represent these processes as pH, DO, and COD were not included in the simulations. However, as the model can successfully simulate the changes in nitrate in time, and since nitrate N was the main source of nitrite N and one of the important sources of ammonia N, a well calibrated nitrate N model is assumed to result in reasonable prediction of nitrite N and ammonia N. Accordingly, nitrite N and ammonia N were calibrated so that the simulated values have the same order of magnitude as the measured (Figures A.1 and A.2).

Results and Discussion

Impacts of projected climate on nitrate N concentrations

The impacts of projected (2020-2050) climate (wet and dry) on surface water nitrate N concentration were determined by comparing the monthly mean concentration of nitrate N of the *baseline A* versus *baseline B* and *C* at stations Fisher, Monticello, and Decatur. In addition, the impacts of projected climate (wet and dry) on soil nitrate N concentration were determined by comparing the monthly mean concentration of nitrate N in unsaturated zone and saturated zone of one cell with continuous corn-soybean crop rotation through the simulation period.

As all the three stations showed the same nitrate tendency and variability, the results from Monticello were used to show how the nitrate N concentration changed on a monthly basis from 1981 to 2015 under the historic and projected climates (Figure 2.5a). The nitrate N NPS concentrations were highest in April and lowest in August in all three stations. Since the dry and

wet climate projections defined the boundary conditions of the future climate projections and nitrate N concentration under historic baseline was within this range, the nitrate N concentration was not expected to change significantly from 2020 to 2050. In addition, due to the high solubility of N NPS, this trend followed the discharge, which was the most dominant factor that controlled N NPS transport under wet projection and historic climate. However, this trend was not expected to hold when the climate became dry (Figure 2.5a). Under dry projection, the nitrate N concentration was higher than baseline and wet projection in February, March, April, and May that the mean nitrate concentrations under dry climate were expected to be around 7.5% higher from February to May compared with the historic baseline. The nitrate N loss was more significant in surface runoff under dry projection due to the decreased precipitation resulting reduced interflow and drainage flow. Under these conditions, the decreasing streamflow offered less dilution resulting in the increased nitrate N concentration in surface water. Furthermore, the month with the highest nitrate N concentration shifted from May to April due to the shift in the peak monthly precipitation from May to April under future projections. This earlier peak in surface water nitrate concentration could cause more potential environmental hazard downstream as the lower temperature in April than May can result in lower nitrate N decay rate allowing for longer residence time. Overall, the nitrate N concentrations in surface water were not expected to change significantly under projected climate if the historic land use was maintained.

In the soil, the effects of climate were consistent. Results showed that the saturated zone nitrate N concentrations were not expected to change significantly under dry projection annually. The unsaturated zone nitrate N concentration, however, was expected to increase by 30% from August to September and decreased by 10% in other months. Under the wet projection, the saturated zone nitrate N concentration showed a 32% increase and the unsaturated zone nitrate N

concentration showed a 200% increase from the historic baseline. These changes were due to the increased infiltration and percolation which brought more nitrate N from the soil upper layers to the lower layers. Overall, these results showed that potential positive impacts might exist in the future due to the higher unsaturated zone nitrate N concentration which can be available for plant use. However, the risk of saturated zone water contamination by nitrate N was expected to increase if climate become wetter.

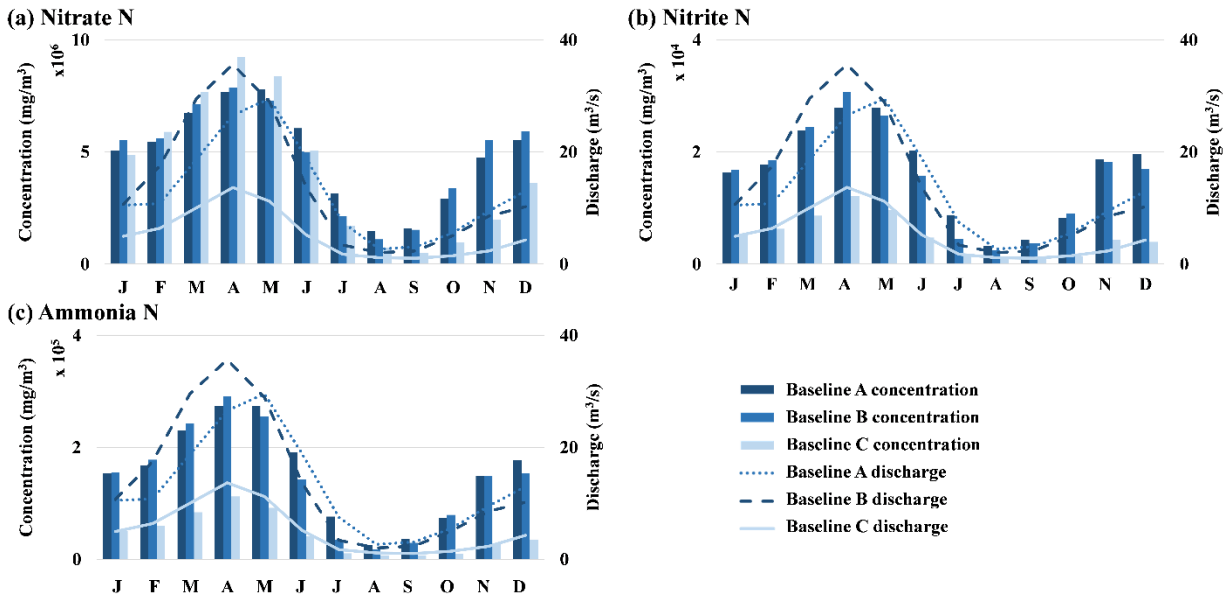

Figure 2.5. Monthly mean N concentrations of (a) nitrate N, (b) nitrite N; (c) ammonia N for the baseline A, baseline B, and baseline C models under three climate projections.

Impacts of projected climate on nitrite and ammonia N concentration in surface water

Unlike nitrate N that was mainly from fertilizer input, all nitrite and ammonia N in the model developed were generated via the N transformation from nitrate fertilizer. It was expected that the nitrite and ammonia N concentrations followed the nitrate N concentration pattern. However, the results (Figure 2.5b and 2.5c) of the simulations showed that the nitrite and ammonia concentrations were driven by the discharge more than the nitrate N concentration. This can be due to the fact that nitrate N was expected to transform into nitrite and ammonia N faster in

surface water than in the unsaturated zone and hence higher discharge could increase the amount of nitrate N that was transformed into other two types of N NPS. However, both types of N NPS concentration were not expected to reach the EPA limit or WHO standards under any climate projections indicating that the agricultural N fertilizer simulated in this research was not able to generate critical nitrite and ammonia concentration in the water. Generally, nitrite N and ammonia N were not expected to post any environmental issues in the USRB under current land use. However, potential risk of high nitrite N and ammonia N concentration still exists if other point sources increase, including urban wastewater discharge, factory wastewater discharges, etc.

Daily nitrate N concentration in surface water

To analyze the monthly behavior of nitrate N concentration in surface water, the probability distribution functions (PDF) of the daily nitrate N concentration were generated. As the behaviors in different months were the same among the stations, the PDFs from Monticello were used as examples to elucidate how nitrate N behaved monthly in surface water.

For nitrate N, the distribution of the daily nitrate showed that there was noticeable probability that the nitrate N to reach "critical" values which exceeded the EPA limit of 10 ppm (mg/L) (USEPA, 2009). Table A.4 showed the probability (rounded to 1%) that the daily nitrate N was higher than the EPA limit for each month. The probability "<1%" in the table meant that the probability was less than 0.5%.

Based on the results, it could be found that the nitrate N concentrations under dry projection was expected to be higher than the concentrations under wet climate projection and historic baseline. The possible reason for this was that the dilution effect from higher discharge under wet projection and historic climate led to lower nitrate N concentration. Furthermore, the month with

the highest probability (50%) was April, which can be due to the bare field conditions prior to plant emergence and high rainfall events producing high surface runoff.

The daily nitrate N concentration distributions by month were found to follow three distinct patterns and were then classified into three categories as “Peak Shape”, “L Shape”, and “Combined Shape”. Three examples were shown in Figure 2.6 representing the months of May, September, and June. The months of February, March, April, and May manifested a “Peak Shape” distribution resembling a near normal distribution (Figure 2.6a). This distribution can be due to the long duration but low intensity rainfall events in these months. As a result, the nitrate N was expected to be transported at a relatively constant rate through the subsurface tile drainage, which formed the peak in the PDF figure. The months of January, July, August, September, October, November, and December showed an “L Shape” distribution where more than 90% of days had a nitrate N concentration less than 1 ppm while less than 5% of days had a nitrate N concentration of more than 9 or 10 ppm. The reason for this nitrate N concentration behavior was due to the short duration but critical rainfall events in these months. The high nitrate N concentrations were expected to be generated only after rainfall events while low nitrate N concentrations were generated consistently during days without critical rainfall events. As a result, the dry days which were usually more than 90% of the days formed the high peak close to zero and the few high values generated by the rainfall events formed the long and low right tail. Finally, for June, the PDF of daily nitrate N concentration showed a “Combined Shape” pattern that had one peak at around 3.5 ppm under future projections and 8 ppm under historic climate and a long and low right tail. As June was in the middle of May with “Peak Shape” and July with “L Shape”, this type of distribution could be viewed as the shift from “Peak Shape” to “L Shape” distribution resulting from the shift in the rainfall pattern.

For nitrite and ammonia N, all the concentrations were lower than either EPA or WHO limits which showed that there was no risk of nitrite and ammonia N from agricultural production becoming a serious environmental problem in the USRB from 2020 to 2050 considering climate changes. The possible reason for this was that the time of concentration for USRB was less than 3 days, which made it impossible to accumulate nitrite and ammonia N in any sections of the river if the source was from the transformation from nitrate. However, potential risk of environmental problems caused by nitrite and ammonia N still existed if additional loads such as point source pollution were discharged into the river.

Overall, the risk of critical nitrate N concentration was expected to be higher when the climate is dry during the seasons when plants were not fully grown while the risk of nitrite and ammonia N in the surface water were not expected to exceed the safety limits. However even under the wettest climate projection, more days with limit-exceeding nitrate N concentration were still expected than the historic climate.

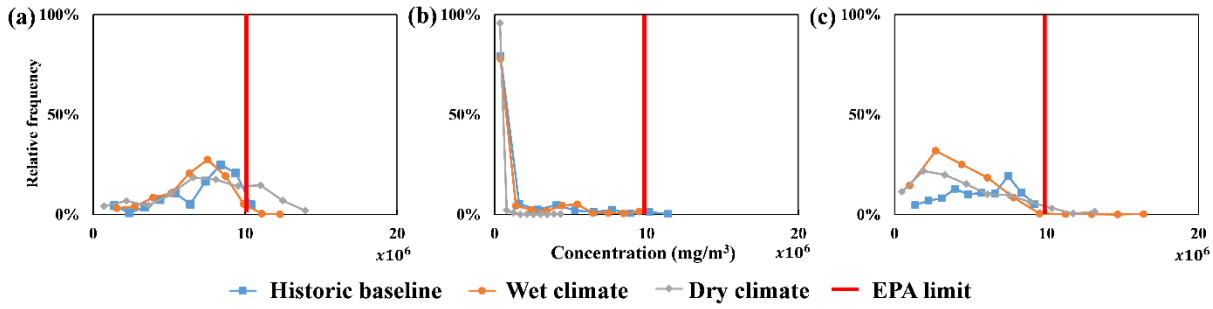

Figure 2.6. Probability distribution functions of different months as examples: (a) May representing "Peak Shape" behavior; (b) September representing "L Shape" behavior; (c) June representing "Combined Shape".

Regulated application rates on NPS in surface water

To compare the effects from regulating fertilizer application amount to 50% of the baseline values to meet the reduction target, the nitrate N concentration at Monticello were compared using scenarios *baseline A*, *regulated A*, *regulated B*, and *regulated C* (Figure 2.7) and the

percentage changes of monthly mean concentrations under wet and dry projections (Figure 2.7b). Because nitrite and ammonia N were transformed from nitrate N and the risk of generating critical nitrite and ammonia N was low in the baseline, the risk of generating critical nitrite N and ammonia N in the scenarios with lower application rates would be even lower sequentially. Hence, it was expected that there was no risk that nitrite and ammonia N transformed from applied nitrate will exceed EPA and WHO limits in scenarios *regulated A, B,* and *C*. These scenarios, with lower application rates, showed significant reduction in nitrate N concentration in all the twelve months but the percentage changes (Figure 2.7b) under different climate projections. The daily nitrate N concentration PDFs of all the twelve months did not exhibit any days that exceeded the EPA limits. The simulations in this research suggested that by regulating the fertilizer application rate to 50% of the original application rate could ensure below critical limits nitrate N concentration all year round.

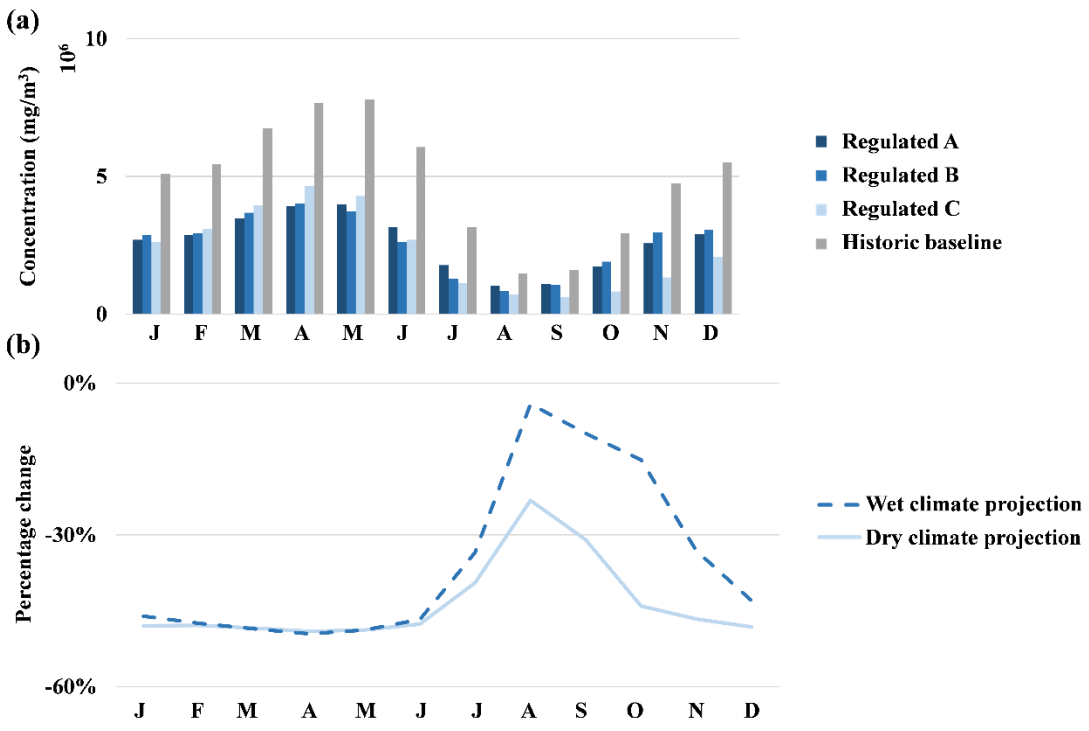

Figure 2.7. (a) Monthly mean nitrate N concentration under three climate projections of scenarios historic baseline, regulated A, regulated B, and regulated C under three climate projections; (b) The monthly mean nitrate concentration percentage changes at Monticello.

Improved cover cropping on nitrate N

To determine the further effects of adopting an updated cover cropping practice under future climate projections when fertilizer application rates were regulated, the nitrate concentration at Monticello from the *regulated (B and C)* and *combined (B and C)* scenarios were evaluated (Figure 2.8). In addition, the nitrate N concentrations on the unsaturated and saturated zones of one sampled cell with continuous corn-soybean crop rotation through the simulation period were compared using the regulated and *combined* (B and C) to determine the effects from improved cover crop land management on nitrate N concentration in the soil (Figure 2.8b and 2.8c). Generally, the reduction in nitrate N concentration was found to be more significant in the surface water and saturated zone than in the unsaturated zone under the dry projection. Under the

dry climate projection, the unsaturated zone nitrate N concentrations did not change significantly compared with the regulated scenario (Figure 2.8b) while both surface water and saturated zone nitrate N concentrations decreased by approximately 33%. In addition, the reduction in surface water nitrate N concentration were the least in July at 7% and became more in the other months. These results were expected given the fact that the grown cover crop could provide additional evapotranspiration from November to March (Figure A.3. 1). The increased evapotranspiration during these months was expected to reduce the percolation to the saturated zone which was expected to decrease the saturated zone nitrate N concentration. As the amount of water and nitrate N concentration in the saturated zone decreased, the drainage flow to the surface water system was expected to decrease as well leading to the decrease in the surface water nitrate N concentration. However, the increase in the infiltration and evapotranspiration in the unsaturated zone were not expected to change the water balance in the unsaturated zone significantly which did not changed unsaturated zone nitrate N concentration significantly.

Under wet climate projection, the nitrate N concentration in the unsaturated zone increased to over 500% from November to April when cover crop was grown and decreased to about 30% from May to October when the main crop was grown (Figure 2.8b). The decrease was only significant in July, August, and September with an average of 7% in surface water. In addition, an average of 33% decrease in saturated zone nitrate N concentration could be expected all year round. From November to April (Figure A.3. 2), the infiltration increased due to higher hydraulic conductivity bringing more nitrate N from soil surface to the unsaturated zone while cover crop resulted in additional evapotranspiration. Based on the results, the change in evapotranspiration was more significant than the change in infiltration which reduced the soil moisture and increased the unsaturated zone nitrate N concentration due to less dilution. The decreased

unsaturated zone soil moisture also reduced the percolation which brought less nitrate N to the saturated zone and reduced drainage flow. In the saturated zone, less nitrate N brought by less percolation reduced the saturated zone nitrate N concentration. At the same time, the decreased drainage flow from saturated zone brought the surface water nitrate N concentration closer to the baseline level even with higher nitrate N concentration in interflow.

From May to October (Figure A.3. 3) when precipitation was high, the increased infiltration and unchanged evapotranspiration were expected to increase percolation and interflow which significantly decreased the unsaturated zone nitrate N concentration (Figure 2.G. 3). Moreover, the percolation also resulted in more drainage flow further decreasing the nitrate N concentration in both the unsaturated and saturated zones. These increased flow from soil to the surface water increased streamflow and decreased the nitrate concentration in surface water. Among the changes, the decrease in the unsaturated zone nitrate N concentration may lead to potential negative impacts for crop growth as the unsaturated zone nitrate N concentration decreased from May to October when the crops were growing (Hansel et al., 2019; Reinbott and Helsel, 1987). However, possible positive effects on crop health existed because cover cropping was expected to improve soil health, reduce pests, and control weeds, which could not be modeled in this research (Bodner et al., 2008; Prunty and Greenland, 1997; Unger and Vigil, 1998). In addition, the increased CO_2 concentration under the extreme projections might also increase the Leaf Area Index (LAI) which in turn was expected to increase evapotranspiration. Increased plant transpiration can decrease soil moisture and can consequently increase the nitrate concentration in soil. However, due to the limitation of the model, this change could not be captured and should also be considered when making land management practices decision.

Overall, the cover cropping was expected to decrease the surface water nitrate N concentrations under dry projection and saturated zone nitrate N concentration under both climate projections. However, potential negative impacts risk for crop growth existed under wet projection due to the lower unsaturated zone nitrate N concentration.

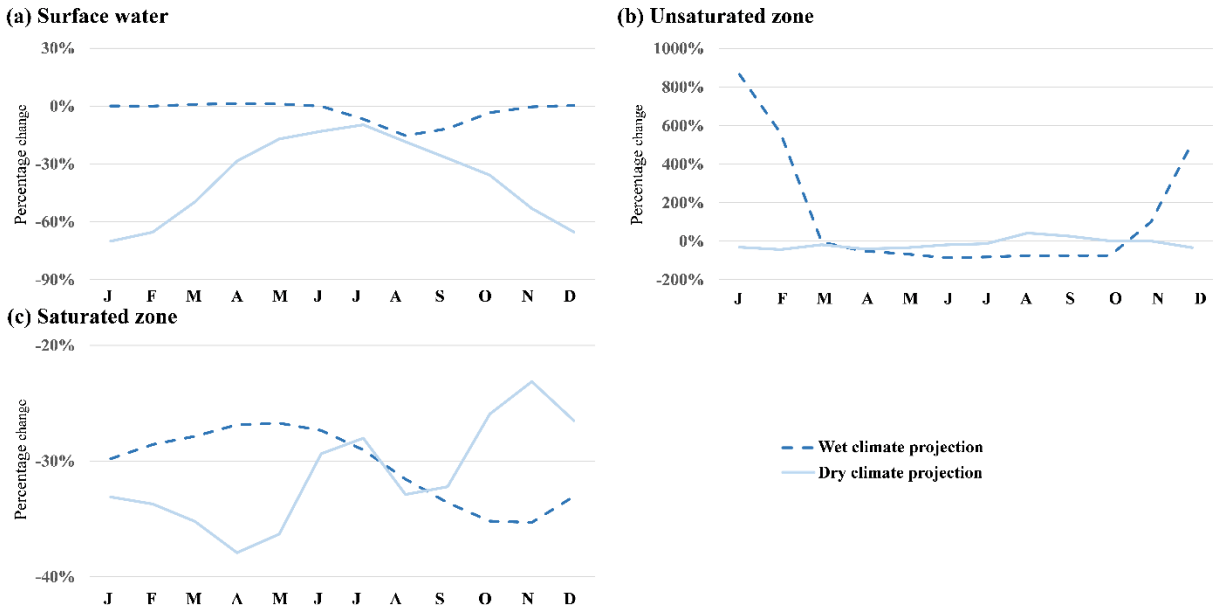

Figure 2.8. The monthly mean nitrate concentration percentage changes under wet and dry projections at Monticello in (a) surface water, (b) unsaturated zone, and (c) saturated zone

Conclusions

The impacts of the different management practices on the fate and transport of nitrate, nitrite, and ammonia N in an intensively managed watershed was simulated using fully distributed physical-based hydrologic and transport models. Management practices such as cover cropping and regulating the fertilizer application rate under wet and dry climate projections were implemented from 2020 to 2050 to determine their effectiveness in reducing the N concentration in surface water and soil. With the current land use and management, the nitrate concentration N in surface water exceeded the EPA limit of 10 ppm (USEPA, 2009) by 2.5% in time. Regulating the fertilizer application rate to approximately 50% of the current rate will ensure that the EPA

limit in surface will not be exceeded in the future under both climate projections. Implementing cover cropping alone can potentially decrease nitrate N concentrations by 33% in surface water under dry climate and in the saturated zone under both wet and dry climate projections. By combining the cover cropping and regulated application rate management, the nitrate N concentration in the saturated zone was expected to decrease by 67% compared with historic baseline, which indicated that combined land management practice could mitigate environmental issues and public health hazards caused by nitrate N contaminated groundwater. Understanding the fate and transport of N in the surface and subsurface domains and their responses to different management and climate regimes can help us formulate the best strategies to reach targeted Nutrient reduction. Similarly, understanding how N transforms into its different components and their subsequent fate in the surface and subsurface zone can help formulate focused adaptation and timely mitigation strategies.

CHAPTER 3: RISK ASSESSMENT OF HARMFUL ALGAL BLOOMS (HAB) OCCURRENCE IN THE AGROECOSYSTEM: A HYDRO-ECOLOGIC MODELING FRAMEWORK AND ENVIRONMENTAL RISK MATRIX.

Introduction

Harmful algal bloom (HAB) is an important environmental concern in the global agroecosystems that can cause large-scale fish kills, decrease aquatic biodiversity, cause odorous water, and result in an overall decline in the ecosystem services that we get from our water bodies (CDC, 2020; USEPA, 2020). Research showed that over 50% of the states in the U.S. are impacted by HAB each year with an economic impact estimated to be over 81 million dollars annually (Anderson et al., 2000; CDC, 2020). High concentration of nitrogen (N) and phosphorus (P) in the surface water, warm water temperature, and low discharge were reported to be the main causes of HAB in freshwater systems (CDC, 2020; USEPA, 2020). HAB in freshwater is typically composed of high density of algae that generates toxins which can potentially harm the health of local communities and freshwater aquatic animals (IDPH, 2020). The HABs caused by certain types of algae such as Golden alga (*Prymnesium parvum*) and Blue-green algae (cyanobacteria) could potentially change the surface watercolor and odor depending on the algae density (Lopez et al., 2008). In Illinois, for example, HABs is often sighted when the weather is warm (e.g., June, July, August, and September) and during the fertilizer application season when nutrient loss is high. Generally, Blue-green algae was the most common cause of HAB in the majority of the U.S. including Illinois freshwater systems (IDPH, 2020; Korppoo et al., 2017). Unsightly and foul-smelling scums, hypoxia, and odorous drinking water were the typical environmental issues caused by blue-green algae related HABs (Lopez et al., 2008). They not only change the color of the water to green but also release toxins including hepatotoxins,

neurotoxins, cytotoxins, dermatotoxins, respiratory, and olfactory irritant toxins (Lopez et al., 2008).

To protect the local public health and agroecosystems, the government typically address the HAB threats by environmental protection plans aimed at lowering the P loads in water bodies since P is the limiting factor for most of the freshwater watersheds in the U.S. (CDC, 2020; Granéli and Turner, 2006; IDPH, 2020). For example, the United States Environmental Protection Agency (U.S.EPA) planned to lower the N and P loads in Illinois by half by 2050 from what they were in 2000 in its "The Gulf Hypoxia Action Plan" (Mississippi River/Gulf of Mexico Watershed Nutrient Task Force, 2008). To meet this goal, research has been conducted to determine if land management practices such as decreasing fertilizer application amount, wetland buffers, and cover crop during field idle time, can be adopted to reduce P load in rivers. Within N and P cycles, P cycle was more difficult to simulate as it was more related to sediment transport than N cycle apart from the drainage flow and surface runoff (Douglas Jr. et al., 1998; Merriman et al., 2019). Constructing wide buffer strips and stabilizing channel banks in the Grand River watershed, southern Ontario, simulated using SWAT, could result to a 50% and 38% decrease in P load in to Lake Erie, respectively (Hanief and Laursen, 2019). Another research also using SWAT showed that agricultural BMPs, including vegetated filter strips, grassed waterways, and reduction of soil-phosphorus concentrations could potentially decrease P load by a maximum of 20% at the watershed outlet (Almendinger and Ulrich, 2017). However, the effectiveness of these practices remained unclear and difficult to evaluate due to the complexities of N and P cycles in water and the lack of proper spatial representation of these cycles in conceptual models like SWAT. For example, particulate P adsorb to sediments were typically estimated as a function of the soil loss which in turn were estimated using empirical

equations like the Universal soil loss equation (USLE) or Revised USLE (RUSLE) (David et al., 2014). In these studies, the use of empirical models was able to closely estimate the general nutrients loss in a state level but did not properly predict the P fate and transport within a watershed nor were they able to assess the effects of field level land management practices on HAB occurrence. To evaluate the occurrence risk of HAB occurrence, a thorough understanding of how the hydrologic processes, climate conditions, and N and P fate and transport can impact HAB is needed if field-level land management practices were considered.

The objective of this research was to assess the occurrence risk of HAB occurrence in a highly cultivated watershed and evaluate the effectiveness of N and P fertilizer reduction land management practices in mitigating this risk under future climate projections. To achieve this objective, a framework was developed for HAB occurrence risk assessment under different environmental stressors including climate changes and different land management practices following four specific objectives: (1) First, a fully distributed physical-based hydrologic model, MIKE SHE, and a hydrodynamic river model, MIKE 11, were coupled with ECO-Lab to simulate the fate and transport of different forms of N and P in the agro-ecosystem in the Upper Sangamon River Basin (USRB), a highly cultivated watershed in central Illinois. (2) Second, the projected N and P concentrations were simulated under the wettest and driest climate projection from 2020 and 2050. (3) The climate change effects on HAB occurrence risk levels were then determined using the simulated N and P concentrations. (4) Finally, two different land management practice scenarios were created based on the government restoration plan on N and P to determine the effectiveness of this restoration plan on HAB occurrence risk levels under extreme climate projections. The growth parameters of blue-green algae were used for algae

growth model to determine the HAB occurrence risk level with N and P concentrations and water temperature (Esteves-Ferreira et al., 2018; Korppoo et al., 2017; Motomura et al., 2018).

Methodology

Study area

The USRB was used as the experiment watershed for model development and P non-point-source pollution fate and transport simulation (Figure 3.1). The USRB, located in central Illinois with an area of approximately 2400 km^2, has more than 84% its land used for agricultural production with corn and soybean to be the most widely grown crops (NRCS, 2017). As the result of its heavily cultivated lands, the USRB has been experiencing environmental problems including high nutrients concentrations and excessive sediments. For example, previous observed data revealed that the nitrate concentration at station Monticello increased by an average of 0.087 mg/L annually in the last 30 years and has exceeded the EPA drinking limits at 10 mg/L since 1980 (Keefer et al., 2010). In addition, the P concentration in USRB has been over the EPA limit of 0.04 ppm since 1980s and algal blooms have been reported occurring in the lakes, river, and ponds in Illinois since then (ILEPA, 2020). To address these environmental concerns and restore the non-market value of the USRB, a project aiming at recovering the water storage of Lake Decatur is currently being implemented. Moreover, land management practices changes aiming at decreasing the N and P concentrations have been included in the Illinois Nutrient Loss Reduction Strategy (ILEPA, 2019).

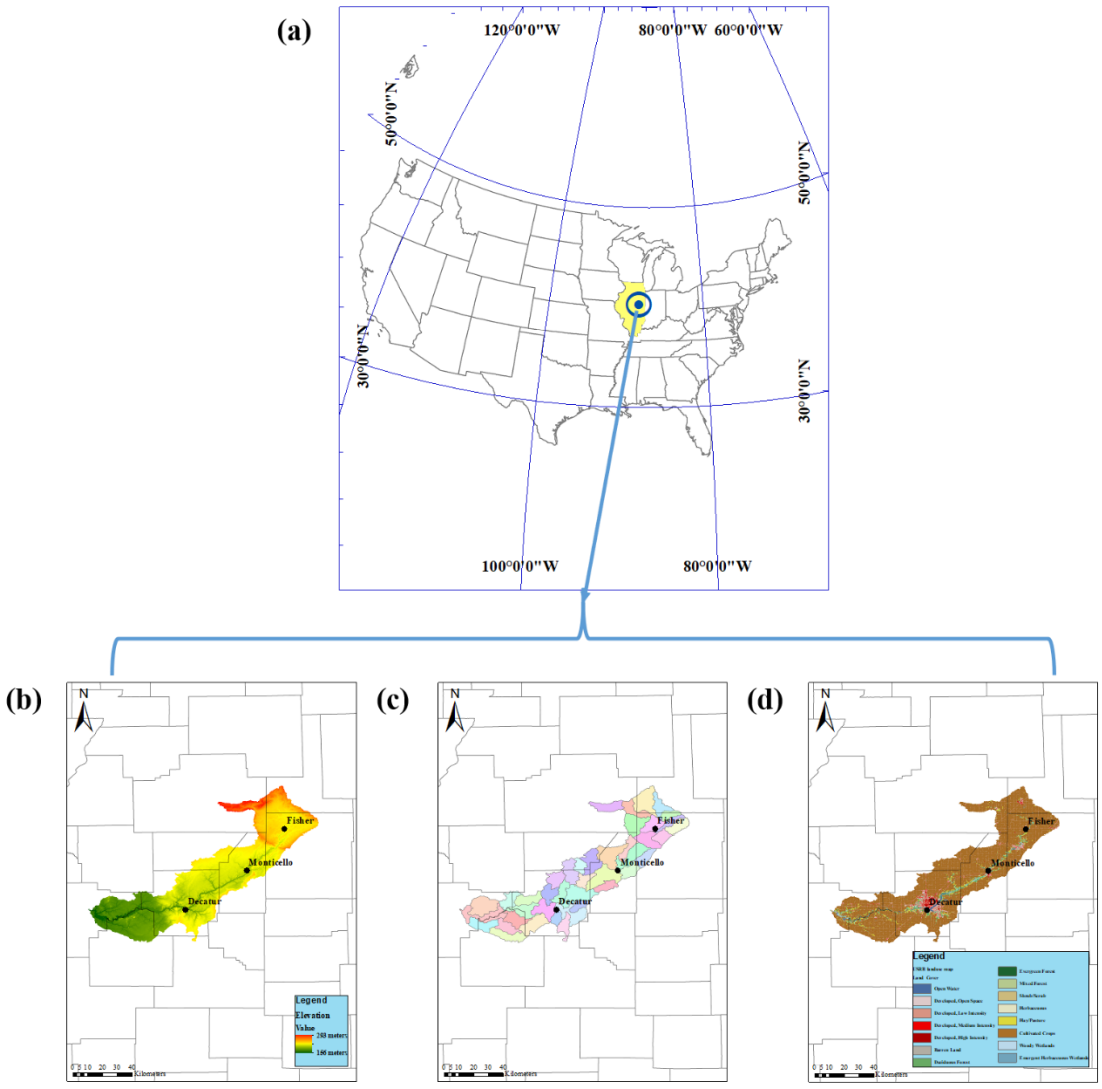

Figure 3.1. The USRB watershed (a) location in the U.S.; (b) digital elevation models (DEM); (c) sub-catchments coverage; (d) land use map.

Nutrient fate and transport models

The water movement and the nutrient cycles were simulated using models MIKE SHE, MIKE 11, and MIKE ECO-Lab. MIKE SHE model, a deterministic physically-based fully distributed model, was used to simulate the hydrologic processes in the surface, unsaturated zone, and saturated zone while MIKE 11, a hydrodynamic 1-D river model, was used to simulate the water movements in the river (DHI, 2017b).

MIKE ECO-Lab, which is an add-on to MIKE SHE and MIKE 11, was used to simulate the N and P cycles in soil and surface water systems (DHI, 2017a). MIKE ECO-Lab N cycle in this research was developed based on the previous research (Hou et al., 2020). The P cycle model was developed using three variables including two types of dissolved phosphorus (DP) and sediment attached phosphorus (SEDP). The two types of DP represented the two types of phosphorus fertilizers that are commonly used in Illinois including Monoammonium Phosphate (MAP) and Ammonium Polyphosphate (APP) whose solubilities are different.

The P cycle model contained two major processes (Figure 3.2): (1) the transformations between MAP and SEDP and that between APP and SEDP which maintained the mass balance of SEDP and DP in the surface water system; and (2) the decay processes of DP representing the crop absorption and natural decay in the unsaturated zone and algae absorption and natural decay in the surface water system. All the DP in the surface water system was considered as the total P that can be consumed by over-growing algae which was referred to as the bioavailable P (BAP). High BAP concentration in surface water was expected to lead to possible algal bloom in the surface water system (Ekholm, 1994; Ellison and Brett, 2006).

The process that MAP and APP were attached to the sediments, the process that SEDP is being released as DP in the surface water, and the decay of DP were governed by first-order exponential decay functions (Eq.3.1 and Eq. 3.2).

$In\frac{C_0}{C} = kt$ (Eq. 3.1)

where C_0 is the state variable concentration at the start of each time step; C is the state variable concentration at the end of each time step; t is the time step; and k is the estimated decay rate for different state variables at temperature, T , computed as follows:

$k = K_{BAP}\ \theta^{T-20}$ (Eq. 3.2)

where K_{BAP} is the estimated BAP decay rate at 20℃ (293.15 K); θ is the estimated temperature correction factor; T is the water temperature for ECO-Lab model for surface water and soil temperature for ECO-Lab model for unsaturated zone and saturated zone.

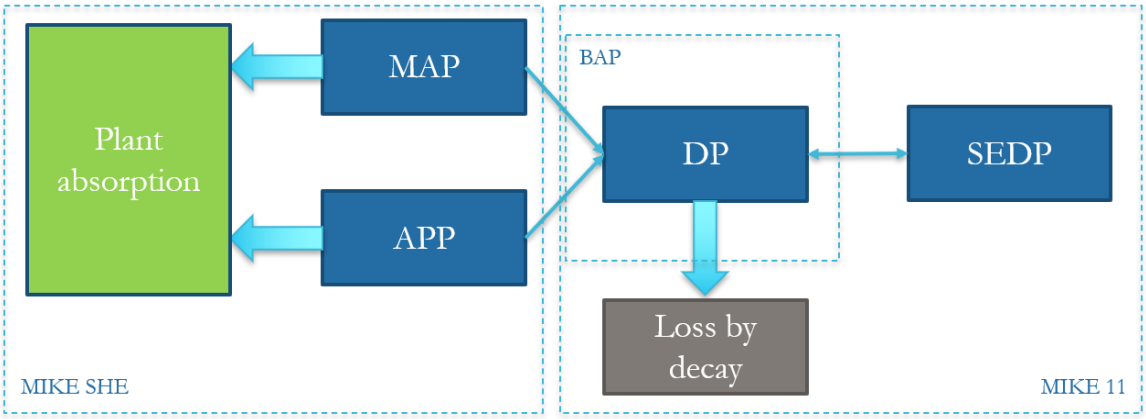

Figure 3.2. P cycle simulated in MIKE ECO-Lab.

Climate projections

The Coupled Model Intercomparison Project phase 5 (CMIP5) from the Working Group on Coupled Modelling (WGCM) of the World Climate Research Programme's (WCRP) was used to generate climate projections (World Climate Research Programme, 2017). The wettest and driest climate projection among the 32 global circulation models (GCMs) under the highest emission level, the Representative Concentration Pathway (RCP) 8.5, were used to simulate the most significant effects from climate changes. Furthermore, these two projections also represented the uncertainty from future climate which can be used to predict the occurrence risk of algal blooms and the distribution of daily N and P concentrations when different land management scenarios were implemented.

P input sources scenario

P in a watershed usually comes from four major sources including agricultural fertilizer application, weathering process from which P is transformed into DP from minerals,

precipitation containing P, and point source P. In this model, all four processes were included as P inputs and expected to contribute to the P simulation in the river as follows:

(1) Fertilizer P application: As P fertilizer application timing and amount in the USRB were not regulated and monitored by any regulatory agencies, the actual P fertilizer application schemes were not available. To correctly simulate and represent the P fertilizer application scenarios, the baseline P fertilizer application rates were based on the recommended rates to maintain the fertilization need in the Illinois Agronomy Handbook and the surveyed crop yield in Illinois by United States Department of Agriculture (USDA) where a five-year-moving average yield was used as the target yield (Hager et al., 2002; USDA, 2020). In addition, the baseline P fertilizer application scenarios were further calibrated based on the measured DP (filtered P in the database) at Fisher and Monticello.

(2) Weathering P: The weathering of P, the process where P is released from apatite minerals and becomes soluble and bioavailable to the ecosystem, is one of the natural DP application process that widely exists (Filippelli, 2002). The natural P weathering processes in the soil were also included in the model based on literature. A supply of 0.0015kg/ha DP per day was evenly applied between the soil surface and 1 m below the surface (Newman, 1995).

(3) Precipitation P: Due to the increased human activities and booming industrial development, the P brought by precipitation cannot be neglected as a source of P and were mainly in soluble or bioavailable form (Ridame and Guieu, 2002). A constant DP concentration of 0.1 g/m^3 was used to represent the input from precipitation (Ridame and Guieu, 2002).

(4) Point source P: Point source P generally was not expected to be significant in most of the watershed as stated in previous research (Liu et al., 2019; Nguyen et al., 2019; Shen et al., 2020). However, the USRB was different due to the existence of the sewage treatment plant

which discharges P load in Decatur (David et al., 2014). To correctly represent the plant discharge, a supply of 3.7kg/ha DP per application was added to the area between Monticello and Decatur in the P fertilizer application scenario.

Model calibration

Model parameters that were not measured or monitored in the field were estimated by calibration. The reaction constant of DP decay, K_{DP} , and the P fertilizer application rates were calibrated and validated based on the sampled DP concentration at Fisher, Monticello, and Decatur from 1978 to 2015 monitored by USGS. The N cycle related parameters were adopted from previous research in the USRB (Hou et al., 2020; USGS, 2019b).

Four periods were used to evaluate the performance of Eco-lab in simulating the different components of the P cycle in USRB: Period 1 (02/14/1979-12/04/1986) at Fisher, period 2 (04/19/2001-10/10/2006) at Monticello, period 3 (08/31/1985-08/01/1987) at Decatur, and period 4 (07/11/1994-06/01/1997) at Decatur were selected for calibration.

Land management practices scenario construction

To address the issues of potential HAB occurrences in the USRB, two different land management scenarios were created aimed at reducing the HAB occurrence risk by decreasing the P or N concentrations in the surface water. These management practices were focused on decreasing fertilizer application rates to determine which type of agricultural fertilizer was more critical in generating HAB.

Previous study showed that the major P source in the USRB was not from nonpoint sources but from the sewage treatment plant locating in the watershed which accounted for about 70% of the total P load (David et al., 2014). Due to the smaller contribution in the total P coming from the

cropping activities, the common land management practices such as cover cropping and crop rotation were not expected to decrease the overall P concentration enough to affect the HAB occurrence risk levels in the USRB. Among the popular practices adapted, decreasing P application rates was proven to be the most efficient and adapted in our simulations (Liu et al., 2019; Merriman et al., 2019).

Similarly for N, previous study in the USRB has shown that decreasing N application by 50% based on the goals in "The Gulf Hypoxia Action Plan", which aimed at decreasing N and P load in the river by 50% by 2050, was expected to lower N concentrations below the EPA standard at 10 ppm (Hou et al., 2020; Mississippi River/Gulf of Mexico Watershed Nutrient Task Force, 2008; USEPA, 2009). The scenarios that met the N goals in this plan were viewed as the best scenarios possible and were adapted in our simulations to determine the effectiveness of N in lowering HAB occurrence risk levels in this watershed. Furthermore, to better understand the effectiveness of the "The Gulf Hypoxia Action Plan" goal in controlling HAB occurrence risks, a combined scenario with both reduced N and P fertilizer application rates was also generated and simulated under the extreme projections (Mississippi River/Gulf of Mexico Watershed Nutrient Task Force, 2008).

To construct the scenarios, the fertilizer N and P application rates were reduced by 50%, while keeping the application timings unchanged from the baseline scenarios. The point sources of N and P were kept unchanged.

BAP behavior under climate change

The BAP stood for all the P that could be used for algae growth in the USRB which is represent by DP in our model. High BAP concentration was expected to lead to the overgrowth of blue-green algae because the requirement of algae was met and longer duration of high BAP

concentrations increased the probability of the overgrowth of algae turning into HAB events (Granéli and Turner, 2006; Lopez et al., 2008). The general behavior of the BAP was evaluated using the following metrics which were simulated under the historic baseline (from 1978 to 2015), wettest, and driest climate projections (from 2020 to 2050) as follows:

(1) The mean BAP concentrations to show the general BAP behavior along the river under climate change.

(2) The percent of days the BAP concentration is higher than the critical BAP concentration for algae growth ($0.2mg/l$) (C. Wang et al., 2016) to show the potential impact from P on algae growth.

(3) The percent of four continuous days with BAP concentration over critical concentration among critical days in category (2) to show the potential occurrence risk of algae fast growth turning into HAB events in the watershed or for downstream if temperature was suitable for HAB. This concept was based on previous research conducted by Beman et al. (2005) which showed that it usually took 3-5 days for a bloom to develop after agricultural runoff with high nutrient concentration discharged to the Gulf of California (Beman et al., 2005; Granéli and Turner, 2006). Based on the research, four continuous days with BAP over the algae growth concentration at $0.2mg/l$ would ensure the occurrence of an HAB event if temperature was suitable.

HAB occurrence risk level assessment

The occurrence risk of HAB occurrence was assessed using the water temperature and bioavailable nutrients concentrations for each scenario simulated. Four HAB occurrence conditions were classified according to the bioavailable nutrients and water temperature (Table 3.1, Figure 3.3). The bioavailable N (BAN) concentration, which was the total concentration of

nitrate and ammonia N, and BAP concentration, which was the DP concentration, were simulated by the Eco-Lab models. The optimal growth concentration (OGC) was the minimum concentration required for exponential growth at half saturation concentration for algal which was $0.2mg/l$ for BAP and $0.8mg/l$ for BAN (Granéli and Turner, 2006; C. Wang et al., 2016). The water temperature factor represented the effects from temperature on HAB growth and the data was simulated by MIKE 11 model which were verified using the downloaded data from USGS. Research showed that HAB species were expected to grow faster than harmless species when water temperature was over $25℃$ and turn general algal blooms (GAB) into HAB (CEES, 2020). As a result, $25℃$ was used as the minimum water temperature for HAB to occur and water temperatures less than $25℃$ would be viewed as the factor leading to potential HAB downstream because the water temperature was expected to be higher in the watersheds downstream of USRB.

Table 3.1. HAB occurrence conditions classified by water temperature and bioavailable nutrient concentrations.

x in $Prob_x$	HAB conditions	Water temperature	Bioavailable nutrient concentrations
1	Potential HAB in USRB	Over 25℃	BAN and BAP concentrations higher than the OGC of HAB
2	Potential HAB in watersheds downstream of USRB	Equal to or less than 25℃	BAN and BAP concentrations higher than the OGC of HAB
3	No potential HAB due to limited P in USRB	Any temperature	BAN higher than the OGC of HAB while BAP lower than the OGC of HAB
4	No potential HAB due to limited N in USRB	Any temperature	BAP higher than the OGC of HAB while BAN lower than the OGC of HAB
5	No potential HAB	Any temperature	BAN and BAP concentrations lower than the OGC of HAB

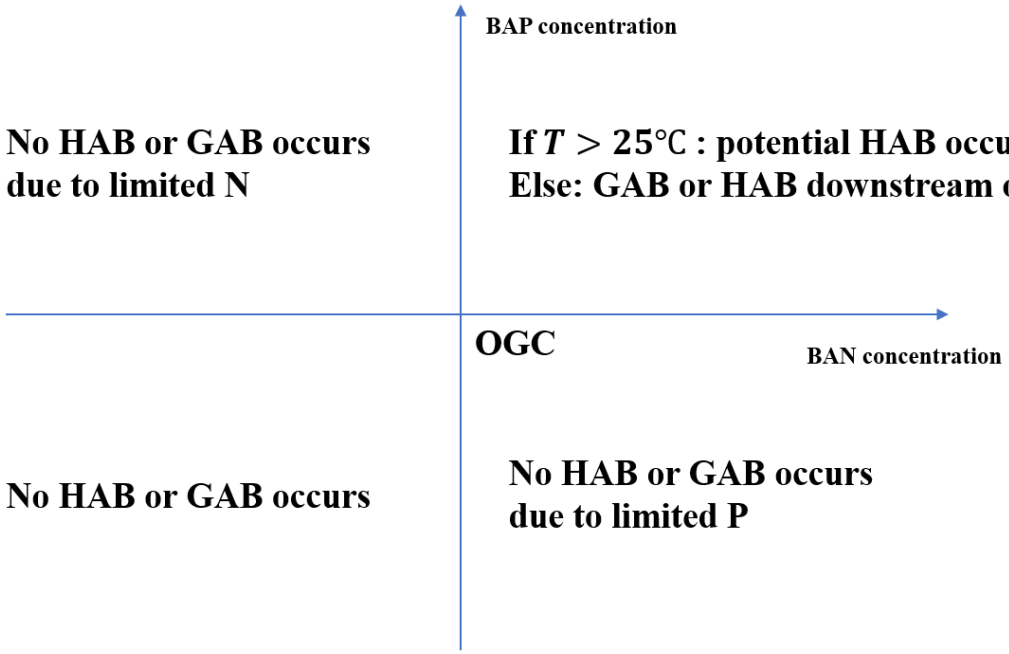

Figure 3.3. The HAB occurrence conditions classified by water temperature, BAN, and BAP.

The Prob_x of HAB condition *x* (Table 3.1) will be used to represent the probabilities of the HAB condition numbered x shown in Table 3.1 and will be calculated as follows:

$$Prob_x = \frac{D_x}{D_{Total}} \text{ (Eq. 3.3)}$$

where D_x is the number of days satisfying condition x in the simulation period and D_{Total} is the total number of days in the simulation period.

Based on the $Prob_x$ calculated, the scenarios with higher $Prob_1$ and lower $Prob_5$ are expected to lead to higher risk of HAB occurrence in the USRB while the scenarios with higher $Prob_2$, $Prob_3$, and $Prob_4$ are expected to result in higher HAB occurrence risk in the watersheds downstream of USRB.

Results and discussion

Calibration

The performance of MIKE ECO-Lab in simulating the P cycle was evaluated by comparing the daily simulated and observed DP at Fisher, Monticello, and Decatur in periods 1 to 4. Since the observed DP concentrations were measured by grab samples, the frequency of the observed data points was sparse and did not allow the computation of performance metrics. Also, as pH, Chemical Oxygen Demand (COD), and Dissolved Oxygen (DO) were not included in the model used, the DP and SEDP simulated were only expected to reflect the general level of P concentrations in the USRB. Considering these factors, the models were calibrated to the level that the daily observed and simulated DP were in the same order of magnitude and the simulated DP followed the general trend of the observed DP (Figure 3.4). Visual inspection of the calibration results (Figure 3.4) suggested that the model was able to replicate the overall behavior of the observed DP in the USRB.

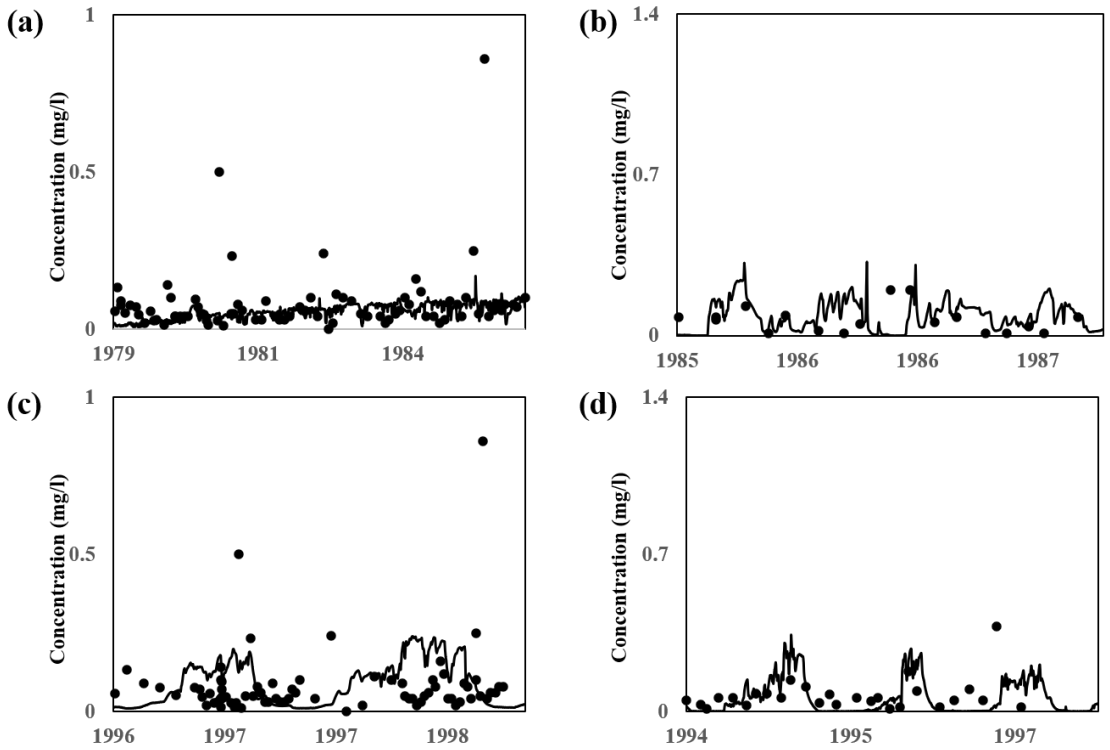

Figure 3.4. The simulated DP concentration time series (line) and observed DP concentrations (point) at (a) Fisher at period 1; (b) Monticello at period 2; (c) Decatur at period 3; and (d) Decatur at period 4.

Impacts of climate on BAP

The impacts of the climate projections on BAP were determined by comparing the effects of the baseline, the wettest, and the driest climate projections on the mean BAP concentrations (Figure 3.5a), percent of days exceeding the critical BAP concentration (Figure 3.5b), and the percent of four continuous days with BAP concentration over critical concentration among critical days (Figure 3.5c) along the main waterway of USRB. The location of three major cities along the river were also labeled including Fisher at around $40km$, Monticello at around $100km$, and Decatur around $149km$ draining 28%, 32%, and 40% of the USRB, respectively (Figure 3.5). Generally, the projected climate (wet and dry) resulted in higher BAP concentrations compared to the historic baseline (Figure 3.5a). The BAP concentrations at the headwater were expected to be higher under dry climate projection than under wet climate projection due to the lack of

precipitation. As river flow passed Monticello ($99.6km$ in Figure 3.5), the extensive P load from surface runoff and leaching under wet climate projection resulted in higher BAP concentration than in the dry climate projection. These findings indicated that BAP concentration was highly dependent on the hydrologic processes (surface runoff and subsurface flow) that were affected by the extreme climate projections.

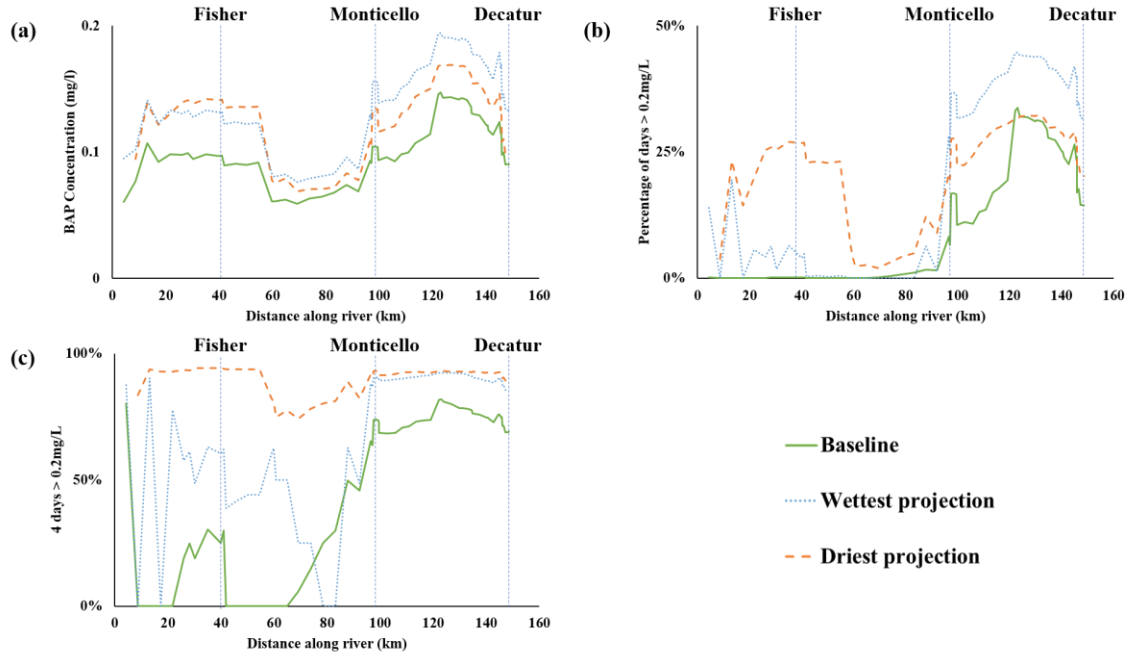

Figure 3.5. The simulated (a) mean BAP concentrations; (b) Percent of days with BAP concentration over critical concentration for algae growth ($0.2mg/l$); (c) Percent of four continuous days with BAP concentrations over critical concentration for algae growth among days in Figure (b).

The number of days with BAP concentration suitable for algae growth also increased under climate projections and more days became suitable for algae growth as climate became drier. This effect was more profound upstream of Monticello due to the significantly low flow. As the difference in percentages was more significant than the difference in mean BAP concentrations between historic baseline and climate projections, more days with extreme high BAP concentrations were expected to happen under the extreme projections. This can be due in part to higher extreme precipitation expected in the projected climates than the historic baseline.

Downstream of Monticello, over 30% of the days under dry projection and over 40% of the days under wet projection were expected to be suitable for algae growth compared with around 15% in historic baseline. This result indicated that the general algae population was expected to be higher in the Upper Sangamon River downstream of Monticello under extreme climate projections. Additionally, not only that the BAP concentrations were more suitable for algae growth, but the high BAP concentrations were expected to have lasted longer than four days, the time needed for existing algae in the river turning into algal blooms. Around 90% of the time, the BAP concentrations in four consecutive days were higher than the critical for algae growth under dry projection. This percentage held the same downstream of Monticello under wet projection. This was because of the slow releasing process of BAP from sediments and the increased amount of sediment washed by extreme precipitation events under extreme climate projections. This process of BAP released by SEDP was expected to last for a long time before the river BAP concentrations returned to a lower value, not optimal for algae growth, and fast flowing water could potentially increase this process by moving BAP to the watershed downstream. The low velocity flow under dry projection was the main reason for the BAP concentrations to be high because it cannot remove enough BAP from the watershed to keep the BAP concentrations at a lower value. This finding indicated that compared with the HAB and GAB occurrence risk in the USRB from 1981 to 2015, more HAB and GAB events were expected to take place when BAP concentrations became critical from 2020 to 2050 under extreme climate projections. Furthermore, the high percentage of days with continuous high BAP concentration meant that the HAB events were expected to last longer if the temperature was suitable for algae growth. Once HAB occurred in the USRB, the events were expected to propagate downstream because of the continuous supply of BAP. This was expected to lead to higher risks for environmental and local

health because the toxins generated by algae were expected to accumulate along the river. Exposure to higher concentration of toxin even for a short period of time (less than one day) was expected to cause serious conditions to aquatic lives and public health (Codd et al., 1999; Geens et al., 2012; Granéli and Turner, 2006).

Overall, BAP behaviors under extreme climate projections were expected to trigger more HAB and GAB events for the USRB and downstream by increasing algae population and the number of days where BAP concentrations are higher than the critical. This condition can be further exacerbated under projected drier climate.

Effects of climate change on HAB occurrence risk

The impacts of the different climate projections on HAB occurrence risk levels were determined by comparing the $Prob_x$ (%) from conditions 1 to 5 (Table 3.1) under the baseline climate, the wettest, and driest climate projections. The $Prob_x$ was computed in spring (*Sp*), summer (*Su*), fall (*Fa*), and winter (*Wi*).

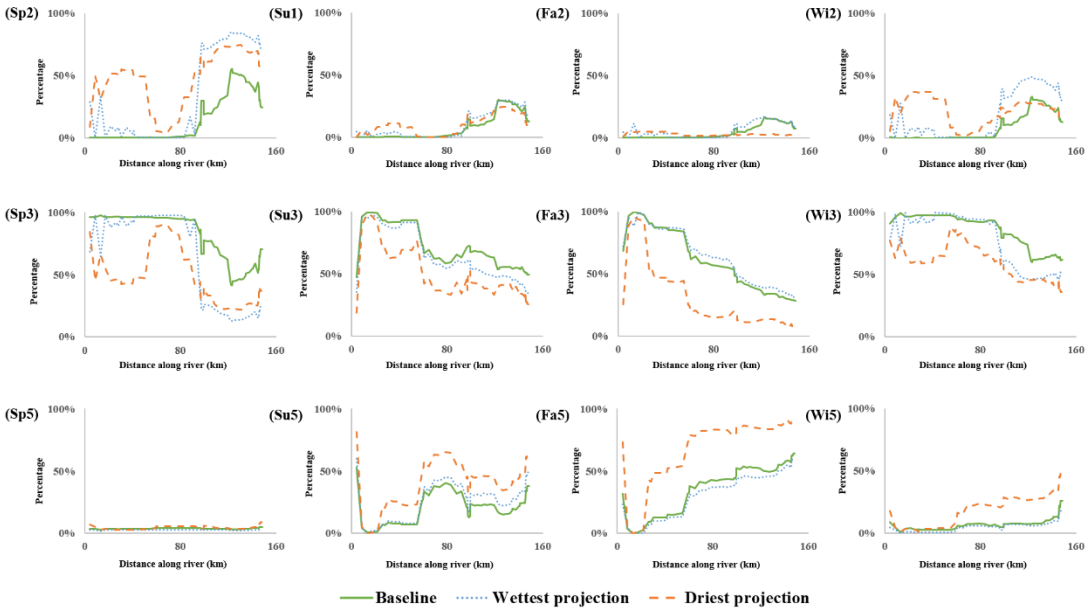

Figure 3.6. $Prob_x$ in each season ($Sp = spring$; $Su = summer$; $Fa = Fall$; $Wi = Winter$) under different projections.

In spring generally, the water temperatures were lower than 25℃ in the USRB which meant that HAB was not expected to happen within the watershed. However, the $Prob_2$, being the probability that HAB was not expected to take place within the USRB due to low water temperature, was the highest. On the other hand, $Prob_5$, which was the probability that HAB would not happen due to the lack of N and P, was the lowest among the four seasons. These results suggested that the watershed downstream was most likely to receive flow with high N and P concentrations from USRB which might trigger GAB or HAB downstream depending on local water temperature (Figure 3.6. Sp2, 3.6. Sp3). This can be due in part to the lack of soil cover during spring prior to the cropping season resulting in higher surface runoff and leaching. The increased in surface runoff and leaching was expected to increase P and N concentrations in the river that can result in high $Prob_2$ in spring.

In summer, the water temperature was likely to reach 25℃ increasing the probability of HAB occurrence in the USRB. In Figure 3.6. Sp1, the $Prob_1$ was unchanged suggesting that climate changes were not expected to change HAB occurrence risks from 2020 to 2050. This trend was due to the droughts in summer under extreme climate changes (Paerl and Otten, 2013). While the extreme precipitation events still existed making the $Prob_1$ the same as historic baseline, drier summer would lead to less N and P loss via surface runoff and leaching. Among N and P, N is more soluble than P which meant more sensitive to droughts. This translated to a higher $Prob_3$ in the baseline than dry and wet projections indicating the historic baseline had more days with high N concentration than extreme projections.

In fall, the water temperatures were not expected to exceed 25℃ resulting in HAB not likely to take place in the USRB. The $Prob_2$ of historic baseline was the same as the $Prob_2$ under wet climate projection and higher than dry climate projection (Figure 3.6. Fa2). This result indicated

that dry climate was expected to lower the GAB and HAB occurrence risk than wet projection in fall due to reduce precipitation and hence lower surface runoff and leaching. Under wet projection, however, the extensive amount of precipitation was expected to generate high surface runoff and leaching with high N and P concentrations even with crop covers.

HAB was not expected to occur in the winter due to low water temperature. The high $Prob_2$ in Figure Wi2 was due mostly from the high precipitation in late winter and early spring along with the melting snow (A. Botero-Acosta et al., 2019). As snow was not expected to generate significant surface runoff in winter, the lower surface runoff from soil significantly decreased the N and P concentrations in river which made the $Prob_5$ highest among all four seasons (Figure 3.6. Wi5).

Overall, HAB occurrence risk was not expected to be high in the USRB mainly because of the low water temperature. The dry climate projection was expected to increase GAB occurrence risk at the headwater if temperatures were suitable and wet climate was expected to increase the GAB or HAB occurrence risk for the watershed downstream. Our results showed that the $Prob_3$ remained high under all extreme climate scenarios and $Prob_4$ were mostly zero. This finding indicated that the USRB was still a P-limited watershed when generating algal blooms even with the sewage treatment plant in the USRB. It can be recalled the USRB is one of the most P-contaminated watersheds in Illinois in which the P yield from the sewage plant was twice as high as the agricultural NPS (David et al., 2014). This conclusion proved that most freshwater watersheds in the U.S. were expected to be P-limited in generating algal blooms and focusing on P reduction is essential in freshwater watershed in decreasing HAB and GAB occurrence risk. This can be because the N fertilizer application rates were much higher than P rates and most of the watershed in Illinois were highly cultivated with corn which is a high N-demanding crop.

Effects of N and P fertilizer application rate reduction on HAB occurrence risk

The impacts of reducing N and P fertilizer application rate on HAB occurrence risk levels were determined by comparing the changes in $Prob_1$ and $Prob_5$ of the N or P fertilizer reduction scenarios from historic baseline under the wettest and driest climate projection (Figure 3.7). Generally, applying N or P fertilizer application rates by 50% separately was expected to offset all the negative effects in generating HAB or GAB under wet projection in summer, fall, and winter because the crop cover along with reduced application rates would significantly decrease the days with critical P or N concentrations. Under dry projection, the reduction was expected to be more significant because surface runoff was much less and crop cover can protect the soil from extreme precipitation events. In spring, the effectiveness of reducing N or P was limited because the extreme precipitation events under climate projections and snow melting were the main causes for the days with high N and P concentrations (Paerl et al., 2016; Paerl and Otten, 2013). The N or P concentrations during those events were usually more than 200% of the critical concentration of $0.2mg/l$ for BAP and $0.8mg/l$ for BAN (Granéli and Turner, 2006; C. Wang et al., 2016). By only reducing N or P fertilizer application rates by 50% were not expected to offset the negative effects from extreme climates.

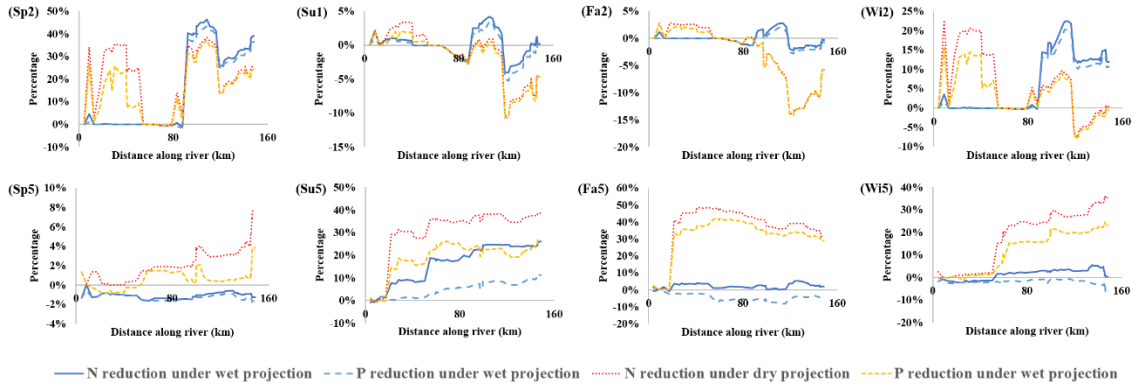

Figure 3.7. $Prob_x$ changes of 50% less N or P fertilizer application rates (projected) land management scenarios in each season ($Sp = spring$; $Su = summer$; $Fa = Fall$; $Wi = Winter$) under different projections from historic baseline.

Between N and P, P was expected to be more effective in reducing HAB or GAB occurrence risk in the USRB because P was the limited factor in this watershed. However, the effectiveness was not as important as expected since the main source of P in the USRB was from point sources. Reducing N, on the other hand, was expected to be more effective in helping control HAB occurrence risk downstream because high N or P concentration from upstream watersheds was expected to fuel HAB in downstream watersheds (Beman et al., 2005).

The combined N and P reduced application rates scenario, however, did not provide any significantly impacts on $Prob_1$ or $Prob_5$ from the scenario with only one type of fertilizer reduced. Generally, the changes brought by adopting reduced rates of the other type of fertilizer after one was reduced were less than 1% and all proved to be not significant because most peaks in N and P were simultaneous and surface runoff and drainage flow were both the main path for BAP and BAN. The only difference was from the slow releasing of DP from SEDP which accounted for the less than 1% changes in $Prob_1$ or $Prob_5$. In addition, more than half of the BAP in the USRB was from point source which meant less related with sediments in the first place because the point-source P load was DP.

Overall, reducing one type of fertilizer by 50% was expected to cancel the negative effects on HAB from extreme climate projection in summer, fall, and winter but could not offset extreme climates in spring. The cancellation effects were expected to become more significant when climate became drier. Regulating N or P fertilizer application rates was expected to increase $Prob_5$ when BAN and BAP were under the OGC. The findings also indicated that regulating P was expected to be more effective in reducing HAB occurrence risk in the USRB while regulating N was more useful in helping downstream control HAB.

Conclusion

The impacts of extreme climate projection and reducing fertilizer application rates on BAP behaviors and HAB occurrence risk level for an intensively managed watershed and downstream was simulated using fully distributed physical-based hydrologic and transport models MIKE SHE/11. Considering BAP, more HAB and GAB events would be triggered for both the USRB and its downstream watersheds due to the increased algae population and longer duration of high BAP occurrence if land managements were kept unchanged from 2020 to 2050 as they were from 1978 to 2015. If temperature was considered, the HAB occurrence risk was not expected to be high in the USRB because of the low water temperature. However, as the N and P concentrations became higher than OGC under wet climate projection, higher HAB occurrence risk is expected downstream side of the USRB due to excessive nutrient loadings. When climate became drier, the HAB occurrence risk was expected to become lower generally but the extreme precipitation events would still generate possible HAB events. Reducing N or P application rates by 50% was found to be effective in offsetting the negative effects of HAB occurrence from extreme climate projections apart from spring. However, regulating the other species of fertilizer after one was not going to change HAB occurrence risk significantly due to the similar behaviors of BAP and BAN during extreme precipitation events. Within P and N, regulating P was more effective in reducing HAB occurrence risks in the USRB while regulating N was more effective in controlling HAB downstream. However, these scenarios required government intervention to regulate fertilizer application during planting seasons and subsidies to maintain the income of farmers which should also be considered by decision-makers.

Our results suggested that P was still the limiting nutrient despite an important P point-source in the USRB. In cases like this, land management practices focusing on P reduction should be

adopted when HAB or GAB occurrences are a concern. Furthermore, more attention should be given during Spring in reducing N and P load in the USRB and possible nutrient reduction practices should be implemented to the downstream watersheds to prevent HAB from lasting longer. The modelling framework developed using MIKE SHE/11 could also be applied to the other watershed to predict and assess the HAB level under other climate projections and field-level land management practices with high temporal resolution. Furthermore, understanding the dynamics of N and P in causing the occurrence of HAB was expected to improve the mitigation measures that we implement at the field level. By being able to simulate field level processes, we can provide better decision-making guidelines that commence at the farms towards the national nutrient reduction target further downstream.

CONCLUSION

Three studies on agricultural nutrients NPS, including nitrogen (N) and phosphorus (P), were simulated and analyzed under different climate projections and land management practices using physically based models. The research tasks developed in this study led to a better understanding of how agricultural nutrients NPS and related environmental issues were impacted by natural and anthropogenic changes such as climate and land management practices. Chapter 1 evaluated the effects of different land management practices on *N* load in surface runoff under future climate projections at the filed scale level. The combinations of land management practices were also evaluated to determine those that can increase productivity with minimal negative impacts on the environment. Moreover, this study developed a methodology to identify areas most vulnerable to generate N load in surface runoff and to target specific management to these areas. Our results also confirmed that fertilizer application rate was the most critical factor in determining both the amount and the probability of high N load. To address this issue, a target application management approach was developed to customize land management practices at the field scale level to reduce the amount and probability of high N load. In the second chapter, the impacts of the different management practices on the fate and transport of nitrate, nitrite, and ammonia N in an intensively managed watershed was simulated using fully distributed physical-based hydrologic and transport models. Understanding the fate and transport of N in the surface and subsurface domains and their responses to different management and climate regimes can help us formulate the best strategies to reach targeted Nutrient reduction. Similarly, understanding how N transforms into its different components and their subsequent fate in the surface and subsurface zone can help formulate focused adaptation and timely mitigation strategies. With N fate and transport simulated in the second chapter, the third chapter focused on the harmful algal

bloom (HAB) occurrence risk level related with extensive amount of N and P load in the river. The impacts of extreme climate projection and reducing fertilizer application rates on bioavailable phosphorus (BAP) behaviors and HAB occurrence risk level for an intensively managed watershed and downstream was also simulated using fully distributed physical-based hydrologic and transport models MIKE SHE/11. Our results suggested that P was still the limiting nutrient despite an important P point-source in the Upper Sangamon River Basin (USRB). In cases like this, land management practices focusing on P reduction should be adopted when HAB or general algal bloom (GAB) occurrences are a concern. Understanding the dynamics of N and P in causing the occurrence of HAB was expected to improve the mitigation measures that we implement at the field level.

With the improved understanding of the relationship between agricultural nutrients NPS and natural and anthropogenic stressors, more specific and effective land management practices targeting the reduction of agricultural nutrients NPS could be applied based on different climate and natural environment characteristics. Furthermore, this study also developed two modelling frameworks focusing on simulating the different agricultural nutrients NPS considering the field level processes. These frameworks can provide a better platform in evaluating the effectiveness of different land management practices in reducing agricultural nutrients NPS. Overall, my research enabled other researchers and decision makers to assess environmental issues risks and compare the tradeoffs between the welfare of agro-ecosystems and economic benefits using models that are closer to reality than empirical models that have been widely used currently.

REFERENCES

Almendinger, J. E., Ulrich, J. S. (2017). Use of SWAT to Estimate Spatial Scaling of Phosphorus Export Coefficients and Load Reductions Due to Agricultural BMPS. *Journal of the American Water Resources Association*, *53*(3), 547–561. https://doi.org/10.1111/1752-1688.12523

Aminot, A., Kérouel, R. (1995). Reference material for nutrients in seawater: stability of nitrate, nitrite, ammonia and phosphate in autoclaved samples. *Marine Chemistry*. https://doi.org/10.1016/0304-4203(95)00004-B

Anderson, D. M., Hoagland, P., Kaoru, Y., White, A. W. (2000). Economic impacts from harmful algal blooms (HABs) in the United States. *National Oceanic And Atmospheric Administration Norman OK National Severe Storms Lab*, (September), No. WHOI-2000-11.

Arnall, B., Hanks, T., Jones, J., Payne, J., Penn, C., Pugh, B., … Zhang, H. (2011). *Oklahoma Forage and Pasture Fertility Guide*. Stillwater. Retrieved from http://npk.okstate.edu/documentation/factsheets/Pasutre Handbook/E-1021web.pdf

Beaulieu, J. J., Tank, J. L., Hamilton, S. K., Wollheim, W. M., Hall, R. O., Mulholland, P. J., … Thomas, S. M. (2011). Nitrous oxide emission from denitrification in stream and river networks. *Proceedings of the National Academy of Sciences of the United States of America*, *108*(1), 214–9. https://doi.org/10.1073/pnas.1011464108

Beman, J. M., Arrigo, K. R., Matson, P. A. (2005). Agricultural runoff fuels large phytoplankton blooms in vulnerable areas of the ocean. *Nature*, *434*(7030), 211–214. https://doi.org/10.1038/nature03370

Bodner, G., Loiskandl, W., Buchan, G., Kaul, H. P. (2008). Natural and management-induced dynamics of hydraulic conductivity along a cover-cropped field slope. *Geoderma*, *146*(1–2),

317–325. https://doi.org/10.1016/j.geoderma.2008.06.012

Botero-Acosta, A., Chu, M. L., Huang, C. (2019). Impacts of environmental stressors on nonpoint source pollution in intensively managed hydrologic systems. *Journal of Hydrology*. https://doi.org/10.1016/j.jhydrol.2019.124056

Botero-Acosta, Alejandra, Chu, M. L., Stumpf, A. J. (2018). Impacts of environmental stressors on the water resources of intensively managed hydrologic systems. *Hydrological Processes*, *32*(19), 2947–2962. https://doi.org/10.1002/hyp.13244

Carvalho, L., Mcdonald, C., de Hoyos, C., Mischke, U., Phillips, G., Borics, G., … Cardoso, A. C. (2013). Sustaining recreational quality of European lakes: Minimizing the health risks from algal blooms through phosphorus control. *Journal of Applied Ecology*, *50*(2), 315–323. https://doi.org/10.1111/1365-2664.12059

CDC. (2020). General Information | Harmful Algal Blooms | CDC. Retrieved March 15, 2020, from https://www.cdc.gov/habs/general.html

CEES. (2020). What causes algal blooms? | Center for Earth and Environmental Science. Retrieved March 16, 2020, from https://cees.iupui.edu/research/algal-toxicology/bloomfactors

Chapman, T. (1999). A comparison of algorithms for streamflow recession and baseflow separation. *Hydrological Processes*, *13*(July 1998), 701–714. https://doi.org/10.1002/(SICI)1099-1085(19990415)13:5<701::AID-HYP774>3.0.CO;2-2

Chen, L., Messing, I., Zhang, S., Fu, B., Ledin, S. (2003). Land use evaluation and scenario analysis towards sustainable planning on the Loess Plateau in China - Case study in a small catchment. *Catena*, *54*(1–2), 303–316. https://doi.org/10.1016/S0341-8162(03)00071-7

Cheng, I. F., Muftikian, R., Fernando, Q., Korte, N. (1997). Reduction of nitrate to ammonia by

zero-valent iron. *Chemosphere*, *35*(11), 2689–2695. https://doi.org/10.1016/S0045-6535(97)00275-0

Cheng, X., Chen, L., Sun, R. (2019). Modeling the non-point source pollution risks by combing pollutant sources, precipitation, and landscape structure. *Environmental Science and Pollution Research*, *26*(12), 11856–11863. https://doi.org/10.1007/s11356-019-04384-y

Codd, G., Bell, S., Kaya, K., Ward, C., Beattie, K., Metcalf, J. (1999). Cyanobacterial toxins, exposure routes and human health. *European Journal of Phycology*, *34*(4), 405–415. https://doi.org/10.1080/09670269910001736462

David, M. B., Mcisaac, G. F., Schnitkey, G. D., Czapar, G. F., Mitchell, C. A. (2014). Science Assessment to Support an Illinois Nutrient Loss Reduction Strategy, 68. Retrieved from http://biogeochemistry.nres.illinois.edu/Biogeochem_lab/Science_documents/Illinois_Science_Assessment_Report_May_6.pdf

DHI. (2017a). MIKE ECO Lab.

DHI. (2017b). Mike She Volume 1: User Guide. The Experts in WATER ENVIRONMENTS. *DHI Software Licence Agreement*, *27*(1), 91–95.

Dinçer, A. R., Kargi, F. (2000). Kinetics of sequential nitrification and denitrification processes. *Enzyme and Microbial Technology*, *27*(1–2), 37–42. https://doi.org/10.1016/S0141-0229(00)00145-9

Dinnes, D. L., Karlen, D. L., Jaynes, D. B., Kaspar, T. C., Hatfield, J. L. (2002). Review and Interpretation: Nitrogen Management Strategies to Reduce Nitrate Leaching in Tile-Drained Midwestern Soils. *Agronomy Journal*, *94*(1), 153–171. https://doi.org/10.2134/agronj2002.0153

Domingues, R. B., Barbosa, A. B., Sommer, U., Galvão, H. M. (2011). Ammonium, nitrate and

phytoplankton interactions in a freshwater tidal estuarine zone: Potential effects of cultural eutrophication. *Aquatic Sciences*, *73*(3), 331–343. https://doi.org/10.1007/s00027-011-0180-0

Douglas Jr., C. L., King, K. A., Zuzel, J. F. (1998). Nitrogen and phosphorus in surface runoff and sediment from a wheat-pea rotation in Northeast Oregon. *Journal of Environmental Quality*, *27*(5), 1170–1177.

Edwards, J., Godsey, C., Raun, B., Taylor, R. (2006). Fall nitrogen requirements for winter wheat, *18*(10).

Ekholm, P. (1994). Bioavailability of phosphorus in agriculturally loaded rivers in southern Finland. *Hydrobiologia*, *287*(2), 179–194. https://doi.org/10.1007/BF00010733

ELD, T. E. of L. D. (2014). A Global Initiative for Sustainable Land Management. Retrieved from www.eld-initiative.org#ecolandeg

Ellison, M. E., Brett, M. T. (2006). Particulate phosphorus bioavailability as a function of stream flow and land cover. *Water Research*, *40*(6), 1258–1268. https://doi.org/10.1016/j.watres.2006.01.016

Esteves-Ferreira, A. A., Inaba, M., Fort, A., Araújo, W. L., Sulpice, R. (2018). Nitrogen metabolism in cyanobacteria: metabolic and molecular control, growth consequences and biotechnological applications. *Critical Reviews in Microbiology*, *44*(5), 541–560. https://doi.org/10.1080/1040841X.2018.1446902

Filippelli, G. M. (2002). The global phosphorus cycle. *Phosphates: Geochemical, Geobiological and Materials Importance*, *48*, 391–426. https://doi.org/10.2138/rmg.2002.48.10

Geens, T., Aerts, D., Berthot, C., Bourguignon, J.-P., Goeyens, L., Lecomte, P., … Covaci, A. (2012). Cyanobacteria Toxins. *Food and Chemical Toxicology Journal*, *50*, 3725–3740.

Granéli, E., Turner, J. T. (2006). *An Introduction to Harmful Algae*. *Ecology of Harmful Algae*. https://doi.org/10.1007/978-3-540-32210-8_1

Guzman, J. A., Chu, M. L., Starks, P. J., Moriasi, D. N., Steiner, J. L., Fiebrich, C. A., McCombs, A. G. (2014). Upper Washita River Experimental Watersheds: Data Screening Procedure for Data Quality Assurance. *Journal of Environment Quality*, *43*(4), 1250. https://doi.org/10.1515/bchm2.1927.163.4-6.229

Hager, A., Hollinger, S. E., Angel, J. R., Kirkpatrick, K., Fleming, E., Ali, S. A., … Nafziger, E. D. (2002). Illinois Agronomy Handbook Estimating Nutrient Availability Soil Analysis. *Illinois Agronomy Handbook*, *65*(12), 1–12. Retrieved from http://extension.cropsciences.illinois.edu/handbook/pdfs/chapter03.pdf%0Ahttp://extension.cropsci.illinois.edu/handbook%0Ahttps://dl.sciencesocieties.org/publications/books/abstracts/acsesspublicati/managingnitroge2/25%0Ahttp://extension.cropsciences.illi

Hanief, A., Laursen, A. E. (2019). Meeting updated phosphorus reduction goals by applying best management practices in the Grand River watershed, southern Ontario. *Ecological Engineering*, *130*, 169–175. https://doi.org/10.1016/j.ecoleng.2019.02.007

Hansel, D. S. S., Schwalbert, R. A., Shoup, D. E., Holshouser, D. L., Parvej, R., Vara Prasad, P. V., Ciampitti, I. A. (2019). A review of soybean yield when double-cropped after wheat. *Agronomy Journal*, *111*(2), 677–685. https://doi.org/10.2134/agronj2018.06.0371

Hockenbury, M. R., Grady, C. P. L. (1977). Inhibition of nitrification: effects of selected organic compounds. *Journal of the Water Pollution Control Federation*, *49*(5), 768–777.

Hou, C., Chu, M. L., Botero-Acosta, A., Guzman, J. A. (2020). Modeling field scale nitrogen non-point source pollution (NPS) fate and transport: Influences from land management practices and climate. *Science of the Total Environment*, (xxxx), 143502.

https://doi.org/10.1016/j.scitotenv.2020.143502

IDPH. (2020). Harmful Algal Blooms (HABs) | IDPH. Retrieved January 11, 2021, from https://www.dph.illinois.gov/topics-services/environmental-health-protection/toxicology/habs

ILEPA. (2019). Illinois Nutrient Loss Reduction Strategy | Illinois CBMP. Retrieved April 6, 2019, from http://www.illinoiscbmp.org/Nutrient-Loss-Reduction-Strategy/

ILEPA. (2020). Blue-Green Algae and Harmful Algal Blooms (HABs) - Algal Bloom. Retrieved December 14, 2020, from https://www2.illinois.gov/epa/topics/water-quality/monitoring/algal-bloom/Pages/default.aspx

IPNI. (2020). Nitrogen Notes. Retrieved March 19, 2020, from http://www.ipni.net/NitrogenNotes

Jamieson, R. C., Gordon, R. J., Tattrie, S. C., Stratton, G. W. (2003). Sources and Persistence of Fecal Coliform Bacteria in a Rural Watershed. *Water Quality Research Journal*, *38*(1), 33–47. https://doi.org/10.2166/wqrj.2003.004

Karlen, D. L., Hurley, E. G., Andrews, S. S., Cambardella, C. A., Meek, D. W., Duffy, M. D., Mallarino, A. P. (2006). Crop rotation effects on soil quality at three northern corn/soybean belt locations. *Agronomy Journal*, *98*(3), 484–495. https://doi.org/10.2134/agronj2005.0098

Keefer, L. L., Bauer, E., Markus., M. (2010). Hydrologic and nutrient monitoring of the Lake Decatur Watershed: Final report 1992-2008, 82.

Kelso, B., Smith, R. V, Laughlin, R. J., Lennox, S. D. (1997). Dissimilatory nitrate reduction in anaerobic sediments leading to river nitrite accumulation. *Appl. Environ. Microbiol.*, *63*(12), 4679–4685. Retrieved from https://aem.asm.org/content/63/12/4679.short

Korppoo, M., Huttunen, M., Huttunen, I., Piirainen, V., Vehviläinen, B. (2017). Simulation of

bioavailable phosphorus and nitrogen loading in an agricultural river basin in Finland using VEMALA v.3. *Journal of Hydrology*, *549*, 363–373. https://doi.org/10.1016/j.jhydrol.2017.03.050

Legates, D. R., McCabe, G. J. (1999). Evaluating the use of "goodness-of-fit" measures in hydrologic and hydroclimatic model validation. *Water Resources Research*, *35*(1), 233–241. https://doi.org/10.1029/1998WR900018

Liu, J., Fu, B., Zhang, C. hu, Wang, Y. kuan. (2019). Modelling spatial variation in the treatment costs of non-point source pollution in mountainous regions of southwest China. *Journal of Mountain Science*, *16*(8), 1901–1912. https://doi.org/10.1007/s11629-018-5051-x

Lopez, C. B., Jewett, E. B., Dortch, Q., Walton, B. T., Hudnell, H. K. (2008). Scientific Assessment of Freshwater Harmful Algal Blooms. *Scientific Assessment of Freshwater Harmful Algal Blooms*, (December), 65.

Lu, C., Tian, H. (2017). Global nitrogen and phosphorus fertilizer use for agriculture production in the past half century: Shifted hot spots and nutrient imbalance. *Earth System Science Data*, *9*(1), 181–192. https://doi.org/10.5194/essd-9-181-2017

McLaren, A. D. (1976). Rate constants for nitrification and denitrification in soils. *Radiation and Environmental Biophysics*, *13*(1), 43–48. https://doi.org/10.1007/BF01323622

Merriman, K. R., Daggupati, P., Srinivasan, R., Hayhurst, B. (2019). Assessment of site-specific agricultural Best Management Practices in the Upper East River watershed, Wisconsin, using a field-scale SWAT model. *Journal of Great Lakes Research*, *45*(3), 619–641. https://doi.org/10.1016/j.jglr.2019.02.004

Mississippi River/Gulf of Mexico Watershed Nutrient Task Force. (2008). Gulf hypoxia action plan - 2008. *Framework*, 62.

Moriasi, D. N., Guzman, J. A., Steiner, J. L., Starks, P. J., Garbrecht, J. D. (2014). Seasonal Sediment and Nutrient Transport Patterns. *Journal of Environment Quality*, *43*(4), 1334. https://doi.org/10.2134/jeq2013.11.0478

Motomura, K., Sano, K., Watanabe, S., Kanbara, A., Gamal Nasser, A. H., Ikeda, T., … Hirota, R. (2018). Synthetic Phosphorus Metabolic Pathway for Biosafety and Contamination Management of Cyanobacterial Cultivation. *ACS Synthetic Biology*, *7*(9), 2189–2198. https://doi.org/10.1021/acssynbio.8b00199

Nakaji, T., Fukami, M., Dokiya, Y., Izuta, T. (2001). Effects of high nitrogen load on growth, photosynthesis and nutrient status of Cryptomeria japonica and Pinus densiflora seedlings. *Trees*, *15*(8), 453–461. https://doi.org/10.1007/s00468-001-0130-x

Nendel, C., Berg, M., Kersebaum, K. C., Mirschel, W., Specka, X., Wegehenkel, M., … Wieland, R. (2011). The MONICA model: Testing predictability for crop growth, soil moisture and nitrogen dynamics. *Ecological Modelling*, *222*(9), 1614–1625. https://doi.org/10.1016/j.ecolmodel.2011.02.018

Newman, E. I. (1995). Phosphorus Inputs to Terrestrial Ecosystems. *Journal of Ecology*, *83*(4), 713–726. Retrieved from https://www.jstor.org/stable/2261638

Nguyen, T. T. N., Némery, J., Gratiot, N., Garnier, J., Strady, E., Tran, V. Q., … Aimé, J. (2019). Phosphorus adsorption/desorption processes in the tropical Saigon River estuary (Southern Vietnam) impacted by a megacity. *Estuarine, Coastal and Shelf Science*, *227*, 106321. https://doi.org/10.1016/j.ecss.2019.106321

NRCS. (2003). *National Range and Pasture Handbook*. Retrieved from https://directives.sc.egov.usda.gov/OpenNonWebContent.aspx?content=17734.wba

NRCS. (2016). Web Soil Survey. Retrieved April 6, 2019, from

https://websoilsurvey.sc.egov.usda.gov/App/WebSoilSurvey.aspx

NRCS. (2017). Land Use - About the Data | NRCS. Retrieved December 12, 2017, from https://www.nrcs.usda.gov/wps/portal/nrcs/detail/national/technical/?cid=stelprdb1083122

Oenema, O., Roest, C. W. J. (1998). Nitrogen and phosphorus losses from agriculture into surface waters; the effects of policies and measures in the Netherlands. *Water Science & Technology*, *37*(3), 19–30. Retrieved from https://watermark.silverchair.com/19.pdf?token=AQECAHi208BE49Ooan9kkhW_Ercy7Dm3ZL_9Cf3qfKAc485ysgAAAd8wggHbBgkqhkiG9w0BBwagggHMMIIByAIBADCCAcEGCSqGSIb3DQEHATAeBglghkgBZQMEAS4wEQQM5DXg1faZeuG0eT7FAgEQgIIBko4Pu8ffjOC19RqmCkOYiE1YJVgeXiS68w5aYK14J3pYb-_c2O_g

Olson, R. A., Kurtz, L. T. (1982). Crop Nitrogen Requirements, Utilization, and Fertilization. In *Nitrogen in Agricultural Systems* (Vol. agronomymo, pp. 437–504). https://doi.org/10.2134/agronmonogr49.c12

Paerl, H. W. (1997). Coastal eutrophication and harmful algal blooms: Importance of atmospheric deposition and groundwater as “new” nitrogen and other nutrient sources. *Limnology and Oceanography*, *42*(5part2), 1154–1165. https://doi.org/10.4319/lo.1997.42.5_part_2.1154

Paerl, H. W., Gardner, W. S., Havens, K. E., Joyner, A. R., McCarthy, M. J., Newell, S. E., … Scott, J. T. (2016). Mitigating cyanobacterial harmful algal blooms in aquatic ecosystems impacted by climate change and anthropogenic nutrients. *Harmful Algae*, *54*, 213–222. https://doi.org/10.1016/j.hal.2015.09.009

Paerl, H. W., Otten, T. G. (2013). Harmful Cyanobacterial Blooms: Causes, Consequences, and Controls. *Microbial Ecology*, *65*(4), 995–1010. https://doi.org/10.1007/s00248-012-0159-y

Pierce, D. W., Cayan, D. R., Thrasher, B. L. (2014). Statistical Downscaling Using Localized Constructed Analogs (LOCA)*. *Journal of Hydrometeorology*, *15*(6), 2558–2585. https://doi.org/10.1175/JHM-D-14-0082.1

Prunty, L., Greenland, R. (1997). Nitrate leaching using two potato-corn N-fertilizer plans on sandy soil. *Agriculture, Ecosystems & Environment*, *65*(1), 1–13. https://doi.org/10.1016/S0167-8809(97)00043-1

PSA, P. S. A. (2017). 2014 Commodity Fact Sheet, *5625*(800), 70–75. https://doi.org/10.1023/2FA-3A1011117412693

Reinbott, T., Helsel, Z. (1987). Intercropping soybean into standing green wheat. *Agronomy Journal*, *79*(5), 886–891. https://doi.org/10.2134/agronj1987.00021962007900050026x

Ridame, C., Guieu, C. (2002). Saharan input of phosphate to the oligotrophic water of the open western Mediterranean sea. *Limnology and Oceanography*, *47*(3), 856–869. https://doi.org/10.4319/lo.2002.47.3.0856

Savino, F., Maccario, S., Migliore, G., Oggero, R., Silvestro, L. (2002). Blue baby syndrome. *Journal of Pediatric Gastroenterology and Nutrition*, *34*(5), 563,573.

Schilling, K. E., Wolter, C. F. (2009). Modeling nitrate-nitrogen load reduction strategies for the des moines river, iowa using SWAT. *Environmental Management*, *44*(4), 671–682. https://doi.org/10.1007/s00267-009-9364-y

Shah, D. B., Coulman, G. A. (1978). Kinetics of nitrification and denitrification reactions. *Biotechnology and Bioengineering*, *20*(1), 43–72. https://doi.org/10.1002/bit.260200105

Shen, T., Tang, Y., Li, Y. J., Liu, Y., Hu, H. (2020). An experimental study about the effects of phosphorus loading in river sediment on the transport of lead and cadmium at sediment-water interface. *Science of the Total Environment*, *720*, 137535.

https://doi.org/10.1016/j.scitotenv.2020.137535

Smil, V. (1999). Nitrogen in crop production: An account of global flows. *Global Biogeochemical Cycles*, *13*(2), 647–662.

Sowers, E., Pan, L., Miller, B. C., Smith, J. L. (1994). (1994) Nitrogen Use Efficiency of Split Nitrogen Applications in Soft White Winter Wheat (AJ), 942–948.

Starks, P. J., Fiebrich, C. A., Grimsley, D. L., Garbrecht, J. D., Steiner, J. L., Guzman, J. A., Moriasi, D. N. (2014). Upper Washita River Experimental Watersheds: Meteorologic and Soil Climate Measurement Networks. *Journal of Environment Quality*, *43*(4), 1239. https://doi.org/10.2134/jeq2013.08.0312

Suárez, L. A. (2005). *PRZM-3, A Model for Predicting Pesticide and Nitrogen Fate in the Crop Root and Unsaturated Soil Zones: Users Manual for Release 3.12.2*.

Timmons, D. R., Burwell, R. E., Holt, R. F. (1973). Nitrogen and phosphorus losses in surface runoff from agricultural land as influenced by placement of broadcast fertilizer. *Water Resources Research*, *9*(3), 658–667. https://doi.org/10.1029/WR009i003p00658

Tuppad, P., Santhi, C., Wang, X., Williams, J. R., Srinivasan, R., Gowda, P. H. (2010). Simulation of conservation practices using the apex model. *Applied Engineering in Agriculture*, *26*(5), 779–794. https://doi.org/10.13031/2013.34947

Turner, N. C. (2004). Agronomic options for improving rainfall-use efficiency of crops in dryland farming systems. *Journal of Experimental Botany*, *55*(407), 2413–2425. https://doi.org/10.1093/jxb/erh154

Unger, P. W., Vigil, M. F. (1998). Cover crop effects on soil water relationships. *Journal of Soil and Water Conservation*, *53*(3), 200–207.

United States Census Bureau. (2019). Census.gov. Retrieved April 6, 2019, from

https://www.census.gov/

University of Oklahoma. (2017). Oklahoma Climatological Survey. Norman, OK: Board of Regents of the University of Oklahoma. Retrieved from http://climate.ok.gov/index.php/site/page/climate_of_oklahoma

USDA. (1997). *Usual Planting and Harvesting Dates for U.S. Field Crops*. Retrieved from https://swat.tamu.edu/media/90113/crops-typicalplanting-harvestingdates-by-states.pdf

USDA. (2010). *National Engineering Handbook Chapter 15 Time of Concentration*.

USDA. (2017). Description of SSURGO Database | NRCS Soils. Retrieved December 12, 2017, from https://www.nrcs.usda.gov/wps/portal/nrcs/detail/soils/survey/geo/?cid=nrcs142p2_053627

USDA. (2019). USDA - National Agricultural Statistics Service Homepage. Retrieved July 21, 2019, from https://www.nass.usda.gov/

USDA. (2020). Crop Production | USDA. Retrieved December 9, 2020, from https://www.usda.gov/topics/farming/crop-production

USEPA. (2009). Nitrogen and Phosphorus in Wadeable Streams.

USEPA. (2018). 4. What are EPA's drinking water regulations for ethylbenzene? Retrieved November 12, 2018, from https://safewater.zendesk.com/hc/en-us/articles/211401718-4-What-are-EPA-s-drinking-water-regulations-for-nitrate-

USEPA. (2019). Water Pollution Search | ECHO | US EPA. Retrieved March 1, 2020, from https://echo.epa.gov/trends/loading-tool/water-pollution-search#navigate

USEPA. (2020). Harmful Algal Blooms | Nutrient Pollution | US EPA. Retrieved March 15, 2020, from https://www.epa.gov/nutrientpollution/harmful-algal-blooms#effect

USGS. (2019a). National Land Cover Database. Retrieved July 21, 2019, from

https://www.usgs.gov/centers/eros/science/national-land-cover-database?qt-science_center_objects=0#qt-science_center_objects

USGS. (2019b). USGS Surface-Water Data for the Nation. Retrieved April 6, 2019, from https://waterdata.usgs.gov/nwis/sw

USGS. (2020). National Hydrography. Retrieved February 24, 2020, from https://www.usgs.gov/core-science-systems/ngp/national-hydrography

VanDyke, L. S., Pease, J. W., Bosch, D. J., Baker, J. C. (1999). Nutrient management planning on four Virginia livestock farms: Impacts on net income and nutrient losses. *Journal of Soil and Water Conservation*, *54*(2), 499–505.

Verhagen, F. J. M., Laanbroek, H. J., Woldendrop, J. W. (1995). Competition for ammonium between plant roots and nitrifying and heterotrophic bacteria and the effects of protozoan grazing. *Plant and Soil*, *170*(2), 241–250. https://doi.org/10.1007/BF00010477

Wang, C., Wang, Z., Wang, P., Zhang, S. (2016). Multiple Effects of Environmental Factors on Algal Growth and Nutrient Thresholds for Harmful Algal Blooms: Application of Response Surface Methodology. *Environmental Modeling and Assessment*, *21*(2), 247–259. https://doi.org/10.1007/s10666-015-9481-3

Wang, Y., Bian, J., Zhao, Y., Tang, J., Jia, Z. (2018). Assessment of future climate change impacts on nonpoint source pollution in snowmelt period for a cold area using SWAT. *Scientific Reports*, *8*(1), 1–13. https://doi.org/10.1038/s41598-018-20818-y

WHO. (2003). *Ammonia in Drinking-water Background document for development of WHO Guidelines for Drinking-water Quality*. Retrieved from http://www.who.int/water_sanitation_health/dwq/ammonia.pdf

Wilhite, M., Epa, I., Walkenbach, A., Epa, I., Riley, A., Grant, I. S. (2015). Illinois Nutrient Loss

Reduction Strategy.

Williams, J. R. (1975). SEDIMENT ROUTING FOR AGRICULTURAL WATERSHEDS. *Journal of the American Water Resources Association*, *11*(5), 965–974. https://doi.org/10.1111/j.1752-1688.1975.tb01817.x

Williams, J. R., Izaurralde, R. C., Williams, C., Steglich, E. M. (2015). *Agricultural Policy/Environmental eXtender Model Theoretical Documentation Version 0806*. Retrieved from https://agrilifecdn.tamu.edu/epicapex/files/2017/03/THE-APEX0806-theoretical-documentation-Oct-2015.pdf

Woodyard, J., Johanning, N., Armstrong, S. (2019a). *Post Corn , Going to Soybean : Use Cereal Rye*.

Woodyard, J., Johanning, N., Armstrong, S. (2019b). *Post Soybean , Going to Corn : Use Oats / Radish*.

World Climate Research Programme. (2017). CMIP5 - Overview. Retrieved December 12, 2017, from https://cmip.llnl.gov/cmip5/index.html?submenuheader=0

Zhang, H., Raun, W. R. (2006). Oklahoma Soil Fertility Handbook 2006, 140.

APPENDIX: SUPPLEMENTAL TABLES AND FIGURES

Table A.1. Adapted corn-soybean crop rotation with cover crop for cells with corn and soybean land use

Original Land Use/Management	Updated land management (spring » summer/fall » winter)
Corn	Oats/Radish » Corn » Cereal Rye
Soybean	Cereal Rye » Soybean » Oats/Radish

Table A.2. Scenarios simulating the impacts of reduced fertilizer application rates and cover cropping in combination with crop rotation under historic and future climate.

Scenario	Application rates (Baseline/Regulated)	Improved cover crop (Yes/No)	Climate projections (Historic[a], wet[b], and dry[b])
Baseline A	Baseline	No	Historic
Baseline B	Baseline	No	Wet
Baseline C	Baseline	No	Dry
Regulated A	Regulated	No	Historic
Regulated B	Regulated	No	Wet
Regulated C	Regulated	No	Dry
Updated A	Baseline	Yes	Historic
Updated B	Baseline	Yes	Wet
Updated C	Baseline	Yes	Dry
Combined A	Regulated	Yes	Historic
Combined B	Regulated	Yes	Wet
Combined C	Regulated	Yes	Dry

a The simulation period is from 1981 to 2015 .

b The simulation period is from 2020 to 2050.

Table A.3. Calibrated reaction constants, k, in the MIKE ECO-Lab model in the different compartments

Reactions	Surface water (day^{-1})	Unsaturated zone (day^{-1})	Saturated zone (day^{-1})	Reaction constant range (day^{-1})
Nitrate decay rate ($k_{Eq.2.1} + k_{Eq.2.2}$)	0.00015	0.0005	0.0001	0-0.12
Nitrite decay rate ($k_{Eq.2.3} + k_{Eq.2.4}$)	0.01	0.01	0.02	0-88.8
Ammonia decay rate ($k_{Eq.2.5} + k_{Eq.2.6}$)	0.005	0.005	0.005	0-0.23
Reaction constant from ammonia to nitrite ($k_{Eq.2.7}$)	0.005	0.005	0.005	0-1.15
Reaction constant from nitrite to nitrate ($k_{Eq.2.8}$)	0.04	0.04	0.03	0-88.8
Reaction constant from nitrate to nitrite ($k_{Eq.2.9}$)	0.05	0.01	0.1	0-0.23
Reaction constant from nitrite to ammonia ($k_{Eq.2.10}$)	0.5	0.4	0.5	0-88.8

Table A.4. Probability of nitrate N concentration exceeding EPA limits under different climate projections at Monticello under historic land use.

Scenario	Probability of nitrate N exceeding EPA limits (10 ppm)					
	Jan	**Feb**	**Mar**	**Apr**	**May**	**Jun**
Baseline A	0%	0%	0%	<1%	2%	0%
Baseline B	0%	<1%	<1%	10%	6%	<1%
Baseline C	14%	15%	26%	50%	37%	5%
	Jul	**Aug**	**Sep**	**Oct**	**Nov**	**Dec**
Baseline A	0%	0%	2%	5%	9%	5%
Baseline B	<1%	0%	0%	6%	9%	5%
Baseline C	0%	0%	0%	2%	5%	11%

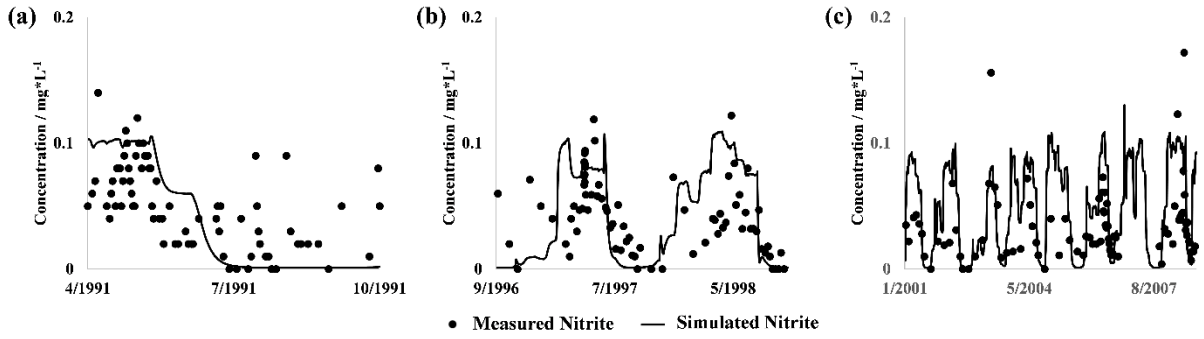

Figure A.1. Observed and simulated nitrite N at four different periods and stations: (a) Period 1 at Monticello; (b) Period 2 at Monticello; and (c) Period 3 at Monticello.

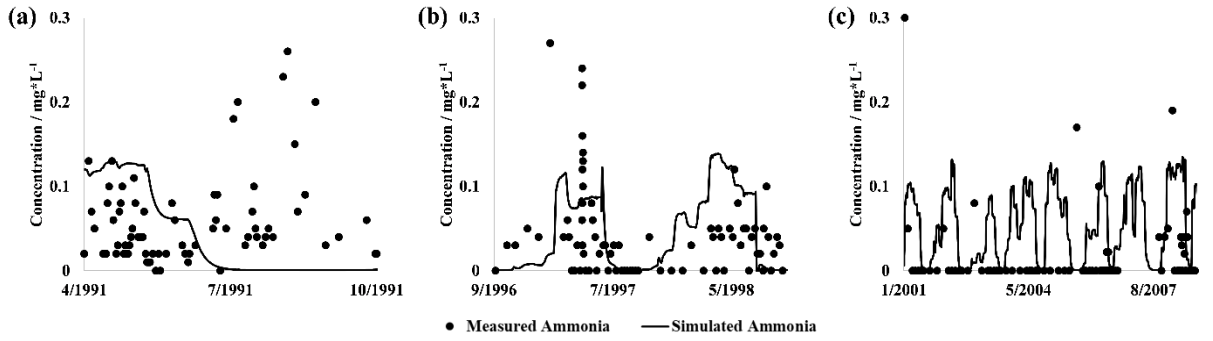

Figure A.2. Observed and simulated ammonia N at three different periods: (a) Period 1 at Monticello; (b) Period 2 at Monticello; and (c) Period 3 at Monticello.

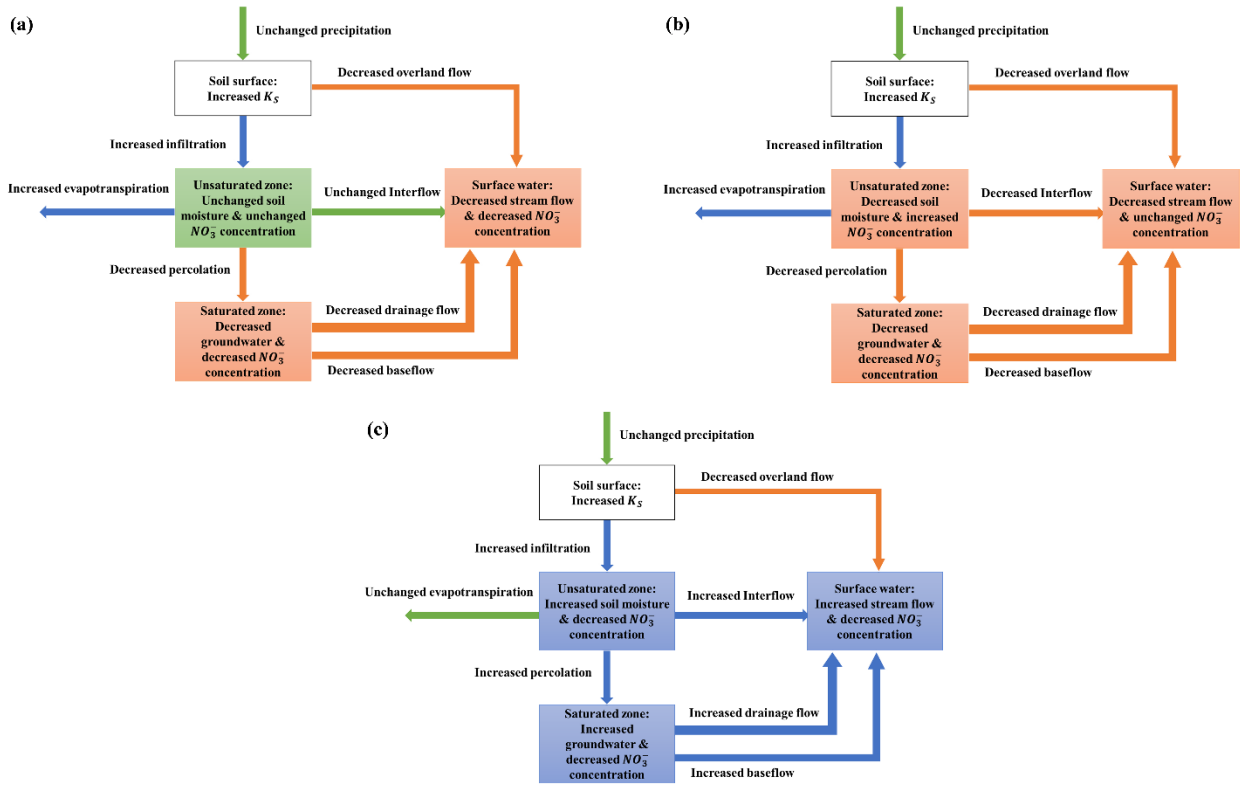

Figure A.3. The changes in flow and nitrate concentration from baseline when applying cover cropping under (a) dry projection, (b) wet projection from November to April, and (3) wet projection from May to October.